

SPECTRAL ACMS: A ROBUST LOCALIZED APPROXIMATED COMPONENT MODE SYNTHESIS METHOD

ALEXANDRE L. MADUREIRA AND MARCUS SARKIS

ABSTRACT. We consider finite element methods of multiscale type to approximate solutions for two-dimensional symmetric elliptic partial differential equations with heterogeneous L^∞ coefficients. The methods are of Galerkin type and follow the Variational Multiscale and Localized Orthogonal Decomposition–LOD approaches in the sense that it decouples spaces into *multiscale* and *fine* subspaces. In a first method, the multiscale basis functions are obtained by mapping coarse basis functions, based on corners used on primal iterative substructuring methods, to functions of global minimal energy. This approach delivers quasi-optimal a priori error energy approximation with respect to the mesh size, but it is not robust with respect to high-contrast coefficients. In a second method, edge modes based on local generalized eigenvalue problems are added to the corner modes. As a result, optimal a priori error energy estimate is achieved which is mesh and contrast independent. The methods converge at optimal rate even if the solution has minimum regularity, belonging only to the Sobolev space H^1 .

1. INTRODUCTION

Let $u : \Omega \rightarrow \mathbb{R}$ be the weak solution of

$$(1) \quad \begin{aligned} -\operatorname{div}(\mathcal{A} \nabla u) &= f \quad \text{in } \Omega, \\ u &= 0 \quad \text{on } \partial\Omega, \end{aligned}$$

where $\Omega \subset \mathbb{R}^2$, and is an open bounded domain with polygonal boundary $\partial\Omega$, the symmetric tensor $\mathcal{A} \in [L^\infty(\Omega)]_{\text{sym}}^{2 \times 2}$ is uniformly positive definite almost everywhere, and $f \in L^2(\Omega)$ is given. For almost all $\mathbf{x} \in \Omega$ let the positive constants a_{\min} and a_{\max} be such that

$$(2) \quad a_{\min}|\mathbf{v}|^2 \leq a_-(\mathbf{x})|\mathbf{v}|^2 \leq \mathcal{A}(\mathbf{x}) \mathbf{v} \cdot \mathbf{v} \leq a_+(\mathbf{x})|\mathbf{v}|^2 \leq a_{\max}|\mathbf{v}|^2 \quad \text{for all } \mathbf{v} \in \mathbb{R}^2,$$

Date: May 19, 2025.

This material is based upon work supported by the National Science Foundation under Grant No. DMS-1929284 while the authors were in residence at the Institute for Computational and Experimental Research in Mathematics in Providence, RI, during the semester program “Numerical PDEs: Analysis, Algorithms, and Data Challenges.” Some of the results were stated without proofs in the conference paper [45]. The first author was supported by the FAPERJ grants E-26/210.128/2022, E-26/211.143.2021, E-26/210.162/2019. The second author was supported by National Science Foundation (Grant No. NSF-MPS 1522663).

where $a_-(\mathbf{x})$ and $a_+(\mathbf{x})$ are the smallest and largest eigenvalues of $\mathcal{A}(\mathbf{x})$. Let $\rho \in L^\infty(\Omega)$ be chosen by the user and such that $\rho(\mathbf{x}) \in [\rho_{\min}, \rho_{\max}]$ almost everywhere for some positive constants ρ_{\min} and ρ_{\max} . Consider g such that

$$f = \rho g,$$

and then the ρ -weighted $L^2(\Omega)$ norm $\|g\|_{L^2_\rho(\Omega)} := \|\rho^{1/2}g\|_{L^2(\Omega)} = \|f\|_{L^2_{1/\rho}(\Omega)}$ is finite. The introduction of the weight ρ is to balance u and f with respect to the tensor \mathcal{A} , adding flexibility to the method and making error estimates more meaningful. It allows for a *fairer measure* of the error when the right hand side of error estimates depends on f only. Also, for high-contrast problems, it might compensate for local low coercivity of \mathcal{A} ; see the end of Section 4 for more details. We note that a related numerical work, without any proofs, was presented in the conference paper [45]. Here the main goal is the corresponding analysis as sharp as possible without any hidden constants.

For $v, w \in H^1(\Omega)$ let

$$a(v, w) = \int_{\Omega} \mathcal{A} \nabla v \cdot \nabla w \, d\mathbf{x},$$

and denote by (\cdot, \cdot) the $L^2(\Omega)$ inner product.

Although in general the solution u of (1) only belongs to the Sobolev space $H^1(\Omega)$, a priori error analyses of multiscale methods established on the literature often rely on solution regularity; see [3, 10, 20, 21, 22, 28, 33, 27, 35, 67, 65] and references therein.

Considering the low contrast case, some methods require minimum regularity, as the generalized finite element methods [2], the rough polyharmonic splines [55], the variational multiscale method [37, 36], the Localized Orthogonal Decomposition (LOD) [53, 52, 50, 51] and the oversampling Multiscale Finite Element Method [32]. The general idea is to decompose the solution spaces as a direct sum of *fine* (local) and *multiscale* (low dimensional, nonlocal) spaces. The final approximate solution belongs to the multiscale space. The LOD approximation [31, 62] also works for the high contrast cases when the local Poincaré inequality is not large; see Remark 1.

However, there are several domain decomposition solvers that are optimal with respect to mesh and contrast, relying on coarse basis functions from local generalized eigenvalue problems. The *adaptive choice of primal constraints* method was introduced to ensure robustness with respect to contrast for non-overlapping domain decomposition methods based on FETI-DP [24, 42] and BDDC [15]. References [4, 9, 14, 56, 39, 40, 41, 48, 49, 47, 54, 70] elaborate on this approach. For overlapping domain decomposition see [16, 23, 25, 39, 69].

Some of these ideas were incorporated in [11, 12] to obtain discretizations that depend only logarithmically on the contrast.

In [46] we introduced the Localized Spectral Decomposition–LSD method for mixed and hybrid-primal methods [64], that is, we re-frame the LOD version in [51] into the non-overlapping domain decomposition framework, and consider the Multiscale Hybrid Method–MHM [1, 28, 29], which falls in the BDDC and FETI-DP classes, and then explore adaptive choice of primal constraints to generate the multiscale basis functions. We obtain a discretization that is robust with respect to contrast.

In this paper we propose an *Approximated Component Mode Synthesis*–ACMS type method; see [6, 7, 13, 30, 33, 34, 38]. The motivation is that known convergence results require extra regularity and are not uniform with respect to contrast [33]. The goal here is to develop a discretization that has optimal and robust a priori error approximation, assuming minimum regularity on the solution, \mathcal{A} and ρ .

To consider the LOD approach with Galerkin-Ritz projection, we use conforming primal iterative substructuring techniques [5, 8, 18, 19, 44, 43, 63, 66, 71] rather than BDDC and FETI-DP methods. Two versions are under consideration here, both of Galerkin type and based on edges and local harmonic extensions. The first method is simpler and converges at quasi-optimal rates, even under minimal regularity of the solution. We note, however, this method has a weak singularity at the coarse nodes and its properties deteriorate if the contrast of the coefficients increases. To circumvent these two issues, we modify the method by incorporating solutions of specially designed local eigenfunction problems, yielding optimal convergence rate uniformly with respect to contrast.

The remainder of this paper is organized as follows. Section 2 describes the substructuring decomposition into interior and interface unknowns, while our methods for low and high contrast coefficients are considered in Sections 3 and 4, respectively. In Section 5 we consider how to deal with local, elementwise problems. Numerical tests and some of the results of this paper, for the case of high-contrast only, were presented without proofs in [45].

2. SUBSTRUCTURING FORMULATION

Let \mathcal{T}_H be a finite element regular partition of Ω based on triangles, with elements of characteristic length $H > 0$. We denote the mesh skeleton by $\partial\mathcal{T}_H$, and denote by \mathcal{N}_H the set of nodes on $\partial\mathcal{T}_H \setminus \partial\Omega$. For $h < H$, let \mathcal{T}_h be a refinement of \mathcal{T}_H , in the sense that every (coarse) edge in $\partial\mathcal{T}_H$ is a union of edges of elements in \mathcal{T}_h . Let \mathcal{N}_h be the set of nodes of \mathcal{T}_h on the skeleton $\partial\mathcal{T}_H \setminus \partial\Omega$. Therefore, all nodes in \mathcal{N}_h belong to edges of elements in \mathcal{T}_H .

For $v \in H^1(\Omega)$ and a given set of elements $\mathcal{T} \subset \mathcal{T}_H$, let

$$|v|_{H_{\mathcal{A}}^1(\Omega)}^2 = \|\mathcal{A}^{1/2} \nabla v\|_{L^2(\Omega)}^2, \quad |v|_{H_{\mathcal{A}}^1(\mathcal{T})}^2 = \sum_{\tau \in \mathcal{T}} \|\mathcal{A}^{1/2} \nabla v\|_{L^2(\tau)}^2.$$

Let $V_h \subset H_0^1(\Omega)$ be the space of continuous piecewise linear functions associated with the fine mesh \mathcal{T}_h . For the sake of reference, let $u_h \in V_h$ such that

$$a(u_h, v_h) = (\rho g, v_h) \quad \text{for all } v_h \in V_h.$$

We assume that u_h approximates u well. Our numerical schemes yield good approximations for u_h without ever computing it. As in [32], we use such solution u_h as a reference to estimate the error $u_h - u_h^{\text{ms}}$. That is a departure from classical results where the error $u - u^{\text{ms}}$ is first estimated. Since u^{ms} requires solving infinite dimensional problems, the u^{ms} is replaced by u_h^{ms} and the error $u^{\text{ms}} - u_h^{\text{ms}}$ is then estimated and which requires again density arguments. In summary, our approach analyze what it is implemented, the analysis is simpler and provides sharper estimates since we just need to estimate the error $u_h - u_h^{\text{ms}}$ rather than estimating the sum of the errors $u - u^{\text{ms}}$ and $u^{\text{ms}} - u_h^{\text{ms}}$.

Assume the decomposition $u_h = u_h^B + u_h^{\mathbb{H}}$ in its bubble and harmonic components, where $u_h^B \in V_h^B$, $u_h^{\mathbb{H}} \in V_h^{\mathbb{H}}$, and

$$\begin{aligned} V_h^B &= \{v_h \in V_h : v_h = 0 \text{ on } \partial\tau, \tau \in \mathcal{T}_H\}, \\ V_h^{\mathbb{H}} &= \{u_h^{\mathbb{H}} \in V_h : a(u_h^{\mathbb{H}}, v_h^B) = 0 \text{ for all } v_h^B \in V_h^B\}, \end{aligned}$$

i.e., $V_h^{\mathbb{H}} = (V_h^B)^{\perp_a}$. It follows immediately from the definitions that

$$(3) \quad a(u_h^{\mathbb{H}}, v_h^{\mathbb{H}}) = (\rho g, v_h^{\mathbb{H}}) \quad \text{for all } v_h^{\mathbb{H}} \in V_h^{\mathbb{H}}, \quad a(u_h^B, v_h^B) = (\rho g, v_h^B) \quad \text{for all } v_h^B \in V_h^B.$$

The problems for the bubble solution u_h^B are local and uncoupled and are considered in Section 5.

We now proceed to approximate $u_h^{\mathbb{H}}$, and start by noting that the functions in $V_h^{\mathbb{H}}$ are uniquely determined by their traces on the boundary of elements in \mathcal{T}_H . Let

$$\Lambda_h = \{v_h|_{\partial\mathcal{T}_H} : v_h \in V_h^{\mathbb{H}}\} \subset H^{1/2}(\partial\mathcal{T}_H),$$

and the *local* discrete-harmonic extension operator $T : \Lambda_h \rightarrow V_h^{\mathbb{H}}$ such that, for $\mu_h \in \Lambda_h$,

$$(4) \quad (T\mu_h)|_{\partial\mathcal{T}_H} = \mu_h, \quad \text{and} \quad a(T\mu_h, v_h^B) = 0 \quad \text{for all } v_h^B \in V_h^B.$$

Define the bilinear forms $s_\tau, s : \Lambda_h \times \Lambda_h \rightarrow \mathbb{R}$ such that, for $\mu_h, \nu_h \in \Lambda_h$,

$$s_\tau(\mu_h, \nu_h) = \int_{\tau} \mathcal{A} \nabla T\mu_h \cdot \nabla T\nu_h d\mathbf{x} \quad \text{for } \tau \in \mathcal{T}_H, \quad s(\mu_h, \nu_h) = \sum_{\tau \in \mathcal{T}_H} s_\tau(\mu_h, \nu_h).$$

Let $\lambda_h = u_h|_{\partial\mathcal{T}_H}$. Then $u_h^{\mathbb{H}} = T\lambda_h$ and

$$(5) \quad s(\lambda_h, \mu_h) = (\rho g, T\mu_h) \quad \text{for all } \mu_h \in \Lambda_h.$$

3. THE LOW-CONTRAST MULTISCALE CASE

We now propose a scheme to approximate (5) based on LOD techniques. Define the fine-scale subspace $\tilde{\Lambda}_h \subset \Lambda_h$ by

$$\tilde{\Lambda}_h = \{\tilde{\lambda}_h \in \Lambda_h : \tilde{\lambda}_h(\mathbf{x}_i) = 0 \text{ for all } \mathbf{x}_i \in \mathcal{N}_H\}.$$

Let the multiscale space $\Lambda_h^{\text{ms}} \subset \Lambda_h$ be such that $\tilde{\Lambda}_h \perp_s \Lambda_h^{\text{ms}}$ and $\Lambda_h = \tilde{\Lambda}_h \oplus \Lambda_h^{\text{ms}}$. Our numerical method is defined by $\lambda_h^{\text{ms}} \in \Lambda_h^{\text{ms}}$ such that

$$(6) \quad s(\lambda_h^{\text{ms}}, \mu_h^{\text{ms}}) = (\rho g, T\mu_h^{\text{ms}}) \quad \text{for all } \mu_h^{\text{ms}} \in \Lambda_h^{\text{ms}},$$

and we set $u_h^{\text{ms}} = T\lambda_h^{\text{ms}}$ as an approximation for $u_h^{\mathbb{H}}$.

To make the definition of Λ_h^{ms} explicit, let the coarse-scale space $\Lambda_H \subset \Lambda_h$ be the trace of piecewise continuous linear functions on the $\partial\mathcal{T}_H$ triangulation. Thus, a function $\lambda_H \in \Lambda_H$ is uniquely determined by its nodal values and is linear on each edge. A basis $\{\theta_H^i\}_{i=1}^{\#\mathcal{N}_H}$ for Λ_H can be obtained by imposing that θ_H^i be continuous and piecewise linear on $\partial\mathcal{T}_H$ and $\theta_H^i(\mathbf{x}_j) = \delta_{ij}$ for all $\mathbf{x}_j \in \mathcal{N}_H$. The support of θ_H^i is on all edges of elements $\tau \in \mathcal{T}_H$ for which $\mathbf{x}_i \in \bar{\tau}$. If $\mu_H = \sum_{i=1}^{\#\mathcal{N}_H} \mu_H(\mathbf{x}_i) \theta_H^i$ is such that $\mu_H(\mathbf{x}_i) = 0$ for all $\mathbf{x}_i \in \mathcal{N}_H$, then $\mu_H(\mathbf{x}) = 0$ for all $\mathbf{x} \in \mathcal{N}_h$. Hence, $\Lambda_h = \Lambda_H \oplus \tilde{\Lambda}_h$, and then $\dim \Lambda_H = \dim \Lambda_h^{\text{ms}}$.

Now, for each $K \in \mathcal{T}_H$ and $\nu_h \in \Lambda_h$, let $P^K : \Lambda_h \rightarrow \tilde{\Lambda}_h$ be such that

$$(7) \quad s(P^K \nu_h, \tilde{\mu}_h) = s_K(\nu_h, \tilde{\mu}_h) \quad \text{for all } \tilde{\mu}_h \in \tilde{\Lambda}_h,$$

and $P : \Lambda_h \rightarrow \tilde{\Lambda}_h$ be such that

$$(8) \quad P\nu_h = \sum_{K \in \mathcal{T}_H} P^K \nu_h.$$

Note that

$$s(P\nu_h, \tilde{\mu}_h) = \sum_{K \in \mathcal{T}_H} s(P^K \nu_h, \tilde{\mu}_h) = \sum_{K \in \mathcal{T}_H} s_K(\nu_h, \tilde{\mu}_h) = s(\nu_h, \tilde{\mu}_h).$$

It follows from the above that $\Lambda_h^{\text{ms}} = \{(I - P)\theta_H^i : \theta_H^i \in \Lambda_H\}$. A basis for Λ_h^{ms} is defined by $\lambda_i^{\text{ms}} = (I - P)\theta_H^i \in \Lambda_h^{\text{ms}}$, and by construction, $\lambda_i^{\text{ms}}(\mathbf{x}_j) = \delta_{ij}$ for all $\mathbf{x}_j \in \mathcal{N}_H$.

An alternative to (6) is to find $\lambda_H \in \Lambda_H$ such that

$$(9) \quad s((I - P)\lambda_H, (I - P)\mu_H) = (\rho g, T(I - P)\mu_H) \quad \text{for all } \mu_H \in \Lambda_H,$$

and then $\lambda_h^{\text{ms}} = (I - P)\lambda_H$. We name it as ACMS-NLOD (*Approximated Component Mode Synthesis Non-Localized Orthogonal Decomposition*) method.

Albeit being well-defined, the method (9) is not “practical”, in the sense that the operators P^K and P are nonlocal, and computing (7) is as hard as solving (1). To circumvent that, we use the fact that the solutions of (7) actually decay exponentially to zero away from K . That allows the definition of a local approximation $P^{K,j}$ for P^K , having support at a patch of width j around K . Next, before proving the exponential decay, we investigate the convergence rates for the ideal nonlocal solution u_h^{ms} .

In what follows, γ_1, γ_2 , etc denote positive constants that do not depend on \mathcal{A}, f, ρ, h and H , depending only on the shape regularity of elements on \mathcal{T}_h and \mathcal{T}_H . Let

$$\kappa = \max_{\tau \in \mathcal{T}_H} \kappa^\tau, \quad \kappa^\tau = \frac{a_{\max}^\tau}{a_{\min}^\tau}, \quad a_{\max}^\tau = \sup_{\mathbf{x} \in \tau} a_+(\mathbf{x}), \quad a_{\min}^\tau = \inf_{\mathbf{x} \in \tau} a_-(\mathbf{x}),$$

$$\rho_{\max}^\tau = \sup_{\mathbf{x} \in \tau} \rho(\mathbf{x}) \quad \text{and} \quad \rho_{\min}^\tau = \inf_{\mathbf{x} \in \tau} \rho(\mathbf{x}).$$

Let us introduce the global Poincaré’s inequality constant $C_{P,G}$ which is the smallest constant such that for all $\mu_h \in \Lambda_h$

$$(10) \quad \|T\mu_h\|_{L_\rho^2(\Omega)} \leq C_{P,G} |T\mu_h|_{H_{\mathcal{A}}^1(\Omega)}.$$

Let us also introduce the local Poincaré’s inequality constant $c_{P,L} = \max_{\tau \in \mathcal{T}_H} c_{P,L}^\tau$, where the $c_{P,L}^\tau$ are the smallest constants such that

$$(11) \quad \|T\tilde{\mu}_h\|_{L_\rho^2(\tau)} \leq c_{P,L}^\tau H |T\tilde{\mu}_h|_{H_{\mathcal{A}}^1(\tau)} \quad \text{for all } \tilde{\mu}_h \in \tilde{\Lambda}_h.$$

Lemma 1. *Let $\tau \in \mathcal{T}_H$ and $c_{P,L}^\tau$ as in (11). Then, an upper bound for $c_{P,L}^\tau$ is given by*

$$(12) \quad (c_{P,L}^\tau)^2 \leq \gamma_1 (1 + \log(H/h)) \frac{\rho_{\max}^\tau}{a_{\min}^\tau}.$$

Proof. Using that $\tilde{\mu}_h$ vanishes at the \mathcal{N}_H nodes, we have [71]

$$\begin{aligned} \|T\tilde{\mu}_h\|_{L_\rho^2(\tau)}^2 &\leq \gamma_1 H^2 \rho_{\max}^\tau \|T\tilde{\mu}_h\|_{L^\infty(\tau)}^2 \\ &\leq \gamma_1 H^2 (1 + \log(H/h)) \rho_{\max}^\tau |T\tilde{\mu}_h|_{H^1(\tau)}^2 \leq \gamma_1 H^2 (1 + \log(H/h)) \frac{\rho_{\max}^\tau}{a_{\min}^\tau} |T\tilde{\mu}_h|_{H_{\mathcal{A}}^1(\tau)}^2. \end{aligned}$$

□

Lemma 2. *Given $\mu_h \in \Lambda_h$ let $I_H\mu_h \in \Lambda_H$ be its Lagrange \mathcal{N}_H -nodal linear interpolation on $\partial\mathcal{T}_H$. Then*

$$(13) \quad |TI_H\mu_h|_{H_{\mathcal{A}}^1(\Omega)}^2 \leq \gamma_2 \kappa (1 + \log(H/h)) |T\mu_h|_{H_{\mathcal{A}}^1(\Omega)}^2.$$

Proof. Let $T_{\mathcal{I}}$ be defined by (4) with $\mathcal{A} = \mathcal{I}$, the identity matrix. We first note that $|T_{\mathcal{I}}\mu_h|_{H^1(\tau)} \leq |T\mu_h|_{H^1(\tau)}$, since $T_{\mathcal{I}}\mu_h$ minimizes $|\cdot|_{H^1(\tau)}$ over all functions in $H^1(\tau)$ with trace equal to μ_h over the element boundary. It follows [71] for each $\tau \in \mathcal{T}_H$ that

$$\begin{aligned} |TI_H\mu_h|_{H^1_{\mathcal{A}}(\tau)}^2 &\leq |T_{\mathcal{I}}I_H\mu_h|_{H^1_{\mathcal{A}}(\tau)}^2 \leq a_{\max}^{\tau} |T_{\mathcal{I}}I_H\mu_h|_{H^1(\tau)}^2 \leq \gamma_2 a_{\max}^{\tau} (1 + \log(H/h)) |T_{\mathcal{I}}\mu_h|_{H^1(\tau)}^2 \\ &\leq \gamma_2 a_{\max}^{\tau} (1 + \log(H/h)) |T\mu_h|_{H^1(\tau)}^2 \leq \gamma_2 \kappa^{\tau} (1 + \log(H/h)) |T\mu_h|_{H^1_{\mathcal{A}}(\tau)}^2. \end{aligned}$$

□

We now extend the *Face Lemma* [71, Subsection 4.6.3] to variable coefficients.

Lemma 3. *Let $\tau \in \mathcal{T}_H$, e an edge of $\partial\tau$ and χ_e be the characteristic function of e being identically equal to one on e and zero on $\partial\tau \setminus e$. Then given $\tilde{\mu}_h \in \tilde{\Lambda}_h$ we have*

$$|T\chi_e\tilde{\mu}_h|_{H^1_{\mathcal{A}}(\tau)}^2 \leq \gamma_3 \kappa^{\tau} (1 + \log(H/h)^2) |T\tilde{\mu}_h|_{H^1_{\mathcal{A}}(\tau)}^2.$$

Proof. We have

$$\begin{aligned} |T\chi_e\tilde{\mu}_h|_{H^1_{\mathcal{A}}(\tau)}^2 &\leq |T_{\mathcal{I}}\chi_e\tilde{\mu}_h|_{H^1_{\mathcal{A}}(\tau)}^2 \leq a_{\max}^{\tau} |T_{\mathcal{I}}\chi_e\tilde{\mu}_h|_{H^1(\tau)}^2 \leq \gamma_3 a_{\max}^{\tau} (1 + \log(H/h))^2 |T_{\mathcal{I}}\tilde{\mu}_h|_{H^1(\tau)}^2 \\ &\leq \gamma_3 a_{\max}^{\tau} (1 + \log(H/h))^2 |T\tilde{\mu}_h|_{H^1(\tau)}^2 \leq \gamma_3 \kappa^{\tau} (1 + \log(H/h))^2 |T\tilde{\mu}_h|_{H^1_{\mathcal{A}}(\tau)}^2. \end{aligned}$$

□

Theorem 4. *Let $\lambda_h = u_h|_{\partial\tau_H}$, and λ_h^{ms} solution of (6). Then $\lambda_h - \lambda_h^{\text{ms}} \in \tilde{\Lambda}_h$ and*

$$|u_h^{\mathbb{H}} - u_h^{\text{ms}}|_{H^1_{\mathcal{A}}(\Omega)} \leq c_{P,L} H \|g\|_{L^2_{\rho}(\Omega)},$$

where we recall that $u_h^{\mathbb{H}} = T\lambda_h$ and $u_h^{\text{ms}} = T\lambda_h^{\text{ms}}$.

Proof. First note that $\lambda_h - \lambda_h^{\text{ms}} \in \tilde{\Lambda}_h$ since it follows from the Galerkin orthogonality that $s(\lambda_h - \lambda_h^{\text{ms}}, \mu_h^{\text{ms}}) = 0$ for all $\mu_h^{\text{ms}} \in \Lambda_h^{\text{ms}}$. Using the local Poincaré's inequality (11) we obtain

$$\begin{aligned} |u_h^{\mathbb{H}} - u_h^{\text{ms}}|_{H^1_{\mathcal{A}}(\Omega)}^2 &= s(\lambda_h - \lambda_h^{\text{ms}}, \lambda_h - \lambda_h^{\text{ms}}) = s(\lambda_h - \lambda_h^{\text{ms}}, \lambda_h) = (\rho g, T(\lambda_h - \lambda_h^{\text{ms}})) \\ &\leq \|g\|_{L^2_{\rho}(\Omega)} \|T(\lambda_h - \lambda_h^{\text{ms}})\|_{L^2_{\rho}(\Omega)} \leq c_{P,L} H \|g\|_{L^2_{\rho}(\Omega)} |T(\lambda_h - \lambda_h^{\text{ms}})|_{H^1_{\mathcal{A}}(\Omega)}, \end{aligned}$$

and the result follows. □

3.1. Decaying Results for Low-Contrast coefficients. We next prove exponential decay of $P^K \nu_h$ for $K \in \mathcal{T}_H$. Denote

$$\mathcal{T}_1(K) = \{K\}, \quad \mathcal{T}_{j+1}(K) = \{\tau \in \mathcal{T}_H : \bar{\tau} \cap \bar{\tau}_j \neq \emptyset \text{ for some } \tau_j \in \mathcal{T}_j(K)\}.$$

The following estimate is fundamental to prove exponential decay.

Lemma 5. *Assume that $K \in \mathcal{T}_H$ and $\nu_h \in \Lambda_h$, and let $\tilde{\phi}_h = P^K \nu_h \in \tilde{\Lambda}_h$. Then, for any integer $j \geq 1$,*

$$|T\tilde{\phi}_h|_{H_{\mathcal{A}}^1(\mathcal{T}_H \setminus \mathcal{T}_{j+1}(K))}^2 \leq 9\alpha |T\tilde{\phi}_h|_{H_{\mathcal{A}}^1(\mathcal{T}_{j+1}(K) \setminus \mathcal{T}_j(K))}^2,$$

where $\alpha = \gamma_3 \kappa (1 + \log(H/h))^2$.

Proof. Choose $\tilde{\nu}_h \in \tilde{\Lambda}_h$ such that $\tilde{\nu}_h|_{\partial\tau} = \tilde{\phi}_h$ if $\tau \in \mathcal{T}_H \setminus \mathcal{T}_{j+1}(K)$, and $\tilde{\nu}_h = 0$ on the remaining edges. We obtain

$$\begin{aligned} |T\tilde{\phi}_h|_{H_{\mathcal{A}}^1(\mathcal{T}_H \setminus \mathcal{T}_{j+1}(K))}^2 &= s_K(\tilde{\nu}_h, \nu_h) - \sum_{\tau \in \mathcal{T}_{j+1}(K) \setminus \mathcal{T}_j(K)} s_{\tau}(\tilde{\nu}_h, \tilde{\phi}_h) = - \sum_{\tau \in \mathcal{T}_{j+1}(K) \setminus \mathcal{T}_j(K)} s_{\tau}(\tilde{\nu}_h, \tilde{\phi}_h) \\ &\leq \sum_{\tau \in \mathcal{T}_{j+1}(K) \setminus \mathcal{T}_j(K)} |T\tilde{\nu}_h|_{H_{\mathcal{A}}^1(\tau)} |T\tilde{\phi}_h|_{H_{\mathcal{A}}^1(\tau)}, \end{aligned}$$

where we used that $s(\tilde{\nu}_h, \tilde{\phi}_h) = s_K(\tilde{\nu}_h, \nu_h) = 0$ since the support of $\tilde{\nu}_h$ does not intersect with K . For each edge e of $\partial\tau$, let χ_e be the characteristic function of e being identically equal to one on e and zero on $\partial\tau \setminus e$. For $\tau \in \mathcal{T}_{j+1}(K) \setminus \mathcal{T}_j(K)$,

$$|T\tilde{\nu}_h|_{H_{\mathcal{A}}^1(\tau)}^2 \leq 3 \sum_{e \subset \partial\tau} |T(\chi_e \tilde{\nu}_h)|_{H_{\mathcal{A}}^1(\tau)}^2 \leq 9\gamma_3 \kappa^{\tau} (1 + \log H/h)^2 |T\tilde{\phi}_h|_{H_{\mathcal{A}}^1(\tau)}^2,$$

where we have used the *Face Lemma* [71, Subsection 4.6.3]. \square

Corollary 6. *Assume that $K \in \mathcal{T}_H$ and $\nu_h \in \Lambda_h$ and let $\tilde{\phi}_h = P^K \nu_h \in \tilde{\Lambda}_h$. Then, for any integer $j \geq 1$,*

$$|T\tilde{\phi}_h|_{H_{\mathcal{A}}^1(\mathcal{T}_H \setminus \mathcal{T}_{j+1}(K))}^2 \leq e^{-\frac{j}{1+9\alpha}} |T\tilde{\phi}_h|_{H_{\mathcal{A}}^1(\mathcal{T}_H)}^2,$$

where α is as in Lemma 5.

Proof. Using Lemma 5 we have

$$|T\tilde{\phi}_h|_{H_{\mathcal{A}}^1(\mathcal{T}_H \setminus \mathcal{T}_{j+1}(K))}^2 \leq 9\alpha |T\tilde{\phi}_h|_{H_{\mathcal{A}}^1(\mathcal{T}_H \setminus \mathcal{T}_j(K))}^2 - 9\alpha |T\tilde{\phi}_h|_{H_{\mathcal{A}}^1(\mathcal{T}_H \setminus \mathcal{T}_{j+1}(K))}^2$$

and then

$$|T\tilde{\phi}_h|_{H_{\mathcal{A}}^1(\mathcal{T}_H \setminus \mathcal{T}_{j+1}(K))}^2 \leq \frac{9\alpha}{1+9\alpha} |T\tilde{\phi}_h|_{H_{\mathcal{A}}^1(\mathcal{T}_H \setminus \mathcal{T}_j(K))}^2 \leq e^{-\frac{1}{1+9\alpha}} |T\tilde{\phi}_h|_{H_{\mathcal{A}}^1(\mathcal{T}_H \setminus \mathcal{T}_j(K))}^2,$$

and the theorem follows. \square

Remark 1. *The α in this paper, defined in Lemma 5, is estimated as the worst case scenario. For particular cases of coefficients \mathcal{A} and ρ , sharper estimates for α can be derived using weighted Poincaré inequalities techniques and partitions of unity that conform with \mathcal{A} in order to avoid large energies on the interior extensions [18, 17, 33, 57, 61, 59, 60, 68]; see [31, 62] for examples.*

Inspired by the exponential decay stated in Corollary 6, we define the operator P^j as follows. First, for a fixed $K \in \mathcal{T}_H$, let

$$\tilde{\Lambda}_h^{K,j} = \{\tilde{\mu}_h \in \tilde{\Lambda}_h : T\tilde{\mu}_h = 0 \text{ on } \mathcal{T}_H \setminus \mathcal{T}_j(K)\}.$$

Given $\mu_h \in \Lambda_h$, define then $P^{K,j}\mu_h \in \tilde{\Lambda}_h^{K,j}$ such that

$$s(P^{K,j}\mu_h, \tilde{\mu}_h) = s_K(\mu_h, \tilde{\mu}_h) \quad \text{for all } \tilde{\mu}_h \in \tilde{\Lambda}_h^{K,j},$$

and let

$$(14) \quad P^j\mu_h = \sum_{K \in \mathcal{T}_H} P^{K,j}\mu_h.$$

We define the approximation $\lambda_H^j \in \Lambda_H$ of λ_H by

$$(15) \quad s((I - P^j)\lambda_H^j, (I - P^j)\mu_H) = (\rho g, T(I - P^j)\mu_H) \quad \text{for all } \mu_H \in \Lambda_H,$$

and then let $\lambda_h^{\text{ms},j} = (I - P^j)\lambda_H^j$ and $u_h^{\text{ms},j} = T\lambda_h^{\text{ms},j}$. We name the scheme as ACMS-LOD (*Approximated Component Mode Synthesis Localized Orthogonal Decomposition*) method.

We now analyze the approximation error of the method, starting by a technical result essential to obtain the final estimate. Let c_γ be a constant depending only on the shape regularity of \mathcal{T}_H such that

$$(16) \quad \sum_{\tau \in \mathcal{T}_H} |v|_{H^1(\mathcal{T}_j(\tau))}^2 \leq (c_\gamma j)^2 |v|_{H^1(\mathcal{T}_H)}^2,$$

for all $v \in H^1(\mathcal{T}_H)$.

Lemma 7. *Consider $\nu_h \in \Lambda_h$ and the operators P defined by (8) and P^j by (14) for $j > 1$. Then*

$$|T(P - P^j)\nu_h|_{H_A^1(\mathcal{T}_H)}^2 \leq (9c_\gamma j \alpha)^2 e^{-\frac{j-2}{1+9\alpha}} |T\nu_h|_{H_A^1(\mathcal{T}_H)}^2.$$

Proof. Let $\tilde{\psi}_h = (P - P^j)\nu_h = \sum_{K \in \mathcal{T}_H} (P^K - P^{K,j})\nu_h$. For each $K \in \mathcal{T}_H$, let $\tilde{\psi}_h^K \in \tilde{\Lambda}_h$ be such that $\tilde{\psi}_h^K|_e = 0$ if e is a face of an element of $\mathcal{T}_j(K)$ and $\tilde{\psi}_h^K|_e = \tilde{\psi}_h|_e$, otherwise. We obtain

$$(17) \quad |T\tilde{\psi}_h|_{H_A^1(\mathcal{T}_H)}^2 = \sum_{K \in \mathcal{T}_H} \sum_{\tau \in \mathcal{T}_H} s_\tau(\tilde{\psi}_h - \tilde{\psi}_h^K, (P^K - P^{K,j})\nu_h) + s_\tau(\tilde{\psi}_h^K, (P^K - P^{K,j})\nu_h).$$

See that the second term of (17) vanishes since

$$\sum_{\tau \in \mathcal{T}_H} s_\tau(\tilde{\psi}_h^K, (P^K - P^{K,j})\nu_h)_{\partial\tau} = \sum_{\tau \in \mathcal{T}_H} s_\tau(\tilde{\psi}_h^K, P^K\nu_h)_{\partial\tau} = 0.$$

For the first term of (17),

$$\begin{aligned} \sum_{\tau \in \mathcal{T}_H} s_\tau(\tilde{\psi}_h - \tilde{\psi}_h^K, (P^K - P^{K,j})\nu_h)_{\partial\tau} &\leq \sum_{\tau \in \mathcal{T}_{j+1}(K)} |T(\tilde{\psi}_h - \tilde{\psi}_h^K)|_{H_{\mathcal{A}}^1(\tau)} |T(P^K - P^{K,j})\nu_h|_{H_{\mathcal{A}}^1(\tau)} \\ &\leq |T\tilde{\psi}_h - \tilde{\psi}_h^K|_{H_{\mathcal{A}}^1(\mathcal{T}_{j+1}(K))} |T(P^K - P^{K,j})\nu_h|_{H_{\mathcal{A}}^1(\mathcal{T}_{j+1}(K))}. \end{aligned}$$

However, proceeding as in the proof of Lemma 5, we gather that

$$|T\tilde{\psi}_h - \tilde{\psi}_h^K|_{H_{\mathcal{A}}^1(\mathcal{T}_{j+1}(K))} \leq 3\alpha^{1/2} |T\tilde{\psi}_h|_{H_{\mathcal{A}}^1(\mathcal{T}_{j+1}(K))}$$

Let $\nu_h^{K,j} \in \tilde{\Lambda}_h^{K,j}$ be equal to zero on all faces of elements of $\mathcal{T}_H \setminus \mathcal{T}_j(K)$ and equal to $P^K\nu_h$ otherwise. Using Galerkin best approximation property and Corollary 6 we obtain

$$\begin{aligned} |T(P^K - P^{K,j})\nu_h|_{H_{\mathcal{A}}^1(\mathcal{T}_{j+1}(K))}^2 &\leq |T(P^K - P^{K,j})\nu_h|_{H_{\mathcal{A}}^1(\mathcal{T}_H)}^2 \leq |T(P^K\nu_h - \nu_h^{K,j})|_{H_{\mathcal{A}}^1(\mathcal{T}_H)}^2 \\ &\leq 9\alpha |TP^K\nu_h|_{H_{\mathcal{A}}^1(\mathcal{T}_H \setminus \mathcal{T}_{j-1}(K))}^2 \leq 9\alpha e^{-\frac{j-2}{1+9\alpha}} |TP^K\nu_h|_{H_{\mathcal{A}}^1(\mathcal{T}_H)}^2. \end{aligned}$$

We gather the above results to obtain

$$\begin{aligned} |T\tilde{\psi}_h|_{H_{\mathcal{A}}^1(\mathcal{T}_H)}^2 &\leq 9\alpha e^{-\frac{j-2}{2(1+9\alpha)}} \sum_{K \in \mathcal{T}_H} |T\tilde{\psi}_h|_{H_{\mathcal{A}}^1(\mathcal{T}_{j+1}(K))} |TP^K\nu_h|_{H_{\mathcal{A}}^1(\mathcal{T}_H)} \\ &\leq 9\alpha e^{-\frac{j-2}{2(1+9\alpha)}} c_\gamma j |T\tilde{\psi}_h|_{H_{\mathcal{A}}^1(\mathcal{T}_H)} \left(\sum_{K \in \mathcal{T}_H} |TP^K\nu_h|_{H_{\mathcal{A}}^1(\mathcal{T}_H)}^2 \right)^{1/2}. \end{aligned}$$

We finally gather that

$$|TP^K\nu_h|_{H_{\mathcal{A}}^1(\mathcal{T}_H)}^2 = s(P^K\nu_h, P^K\nu_h)_{\partial\mathcal{T}_H} = s_K(P^K\nu_h, \nu_h) = \int_K \mathcal{A} \nabla(TP^K\nu_h) \cdot \nabla T\nu_h \, d\mathbf{x}$$

and from Cauchy–Schwarz, $|TP^K\nu_h|_{H_{\mathcal{A}}^1(\mathcal{T}_H)} \leq |T\nu_h|_{H_{\mathcal{A}}^1(K)}$, we have

$$\sum_{K \in \mathcal{T}_H} |TP^K\nu_h|_{H_{\mathcal{A}}^1(\mathcal{T}_H)}^2 \leq |T\nu_h|_{H_{\mathcal{A}}^1(\mathcal{T}_H)}^2.$$

□

Theorem 8. Define $u_h^{\mathbb{H}}$ by (3) and let $u_h^{\text{ms},j} = T(I - P^j)\lambda_H^j$, where λ_H^j is as in (15). Then

$$|u_h^{\mathbb{H}} - u_h^{\text{ms},j}|_{H_{\mathcal{A}}^1(\mathcal{T}_H)} \leq H \{ c_{P,L} + [\gamma_2 \kappa (1 + \log(H/h))]^{1/2} c_\gamma j 9\alpha e^{-\left(\frac{j-2}{2(1+9\alpha)} - \log(c_{P,G}/H)\right)} \|g\|_{L_p^2(\Omega)} \}.$$

Proof. First, from the triangle inequality,

$$|u_h^{\mathbb{H}} - u_h^{\text{ms,j}}|_{H_{\mathcal{A}}^1(\mathcal{T}_H)} \leq |u_h^{\mathbb{H}} - u_h^{\text{ms}}|_{H_{\mathcal{A}}^1(\mathcal{T}_H)} + |u_h^{\text{ms}} - u_h^{\text{ms,j}}|_{H_{\mathcal{A}}^1(\mathcal{T}_H)},$$

and for the first term we use Theorem 4. For the second term, we first define $\hat{u}_h^{\text{ms,j}} = \sum_i \lambda_h^{\text{ms}}(\mathbf{x}_i) T(I - P^j) \theta_H^i$, and then

$$u_h^{\text{ms}} - \hat{u}_h^{\text{ms,j}} = T(P - P^j) \sum_i \lambda_h^{\text{ms}}(\mathbf{x}_i) \theta_H^i = T(P - P^j) I_H \lambda_h^{\text{ms}},$$

where I_H is as in Lemma 2. Relying on the Galerkin best approximation we gather from Lemma 7 that

$$|u_h^{\text{ms}} - u_h^{\text{ms,j}}|_{H_{\mathcal{A}}^1(\mathcal{T}_H)}^2 \leq |u_h^{\text{ms}} - \hat{u}_h^{\text{ms,j}}|_{H_{\mathcal{A}}^1(\mathcal{T}_H)}^2 \leq (c_\gamma j)^2 (9\alpha)^2 e^{-\frac{j-2}{(1+9\alpha)}} |T I_H \lambda_h^{\text{ms}}|_{H_{\mathcal{A}}^1(\mathcal{T}_H)}^2.$$

Since $u_h^{\text{ms}} = T \lambda_h^{\text{ms}}$ the result follow from Lemma 2 and the global Poincaré's inequality (10). \square

Remark 2. *Note that nothing precludes the use of quadrilateral meshes and other discretization schemes (hp for instance), but some of the constants in the error estimates would change accordingly.*

4. THE HIGH-CONTRAST MULTISCALE CASE

The main bottle-neck in dealing with high-contrast coefficients is that α becomes too large, therefore j has to be large as well, cf. Theorems 4 and 8. Furthermore, the large local Poincaré inequality constant $c_{P,L}^\tau$ deteriorates the a priori error estimate in Theorem 4. Also, we would like to remove the $(1 + \log(H/h))$ term that appears in these estimates due to the mismatch between $H^{1/2}(e)$ and $H_{00}^{1/2}(e)$ (see [71] for a definition). To deal with these issues, we replace $\tilde{\Lambda}_h$ by a subspace $\Lambda_h^\Delta \subset \tilde{\Lambda}_h$ by removing a subspace spanned by some eigenfunctions associated to an appropriate generalized eigenvalue problem, on each edge of the mesh \mathcal{T}_H . We first introduce some notation.

Given an edge e of an element $\tau \in \mathcal{T}_H$, let $\tilde{\Lambda}_h^e = \tilde{\Lambda}_h|_e$ and $\tilde{\Lambda}_h^\tau = \tilde{\Lambda}_h|_{\partial\tau}$ be the restrictions of functions on $\tilde{\Lambda}_h$ to e and on $\tilde{\Lambda}_h$ to $\partial\tau$. Since $\tilde{\mu}_h^e \in \tilde{\Lambda}_h^e$ vanishes at the end-points of e , it is possible to continuously extend it by zero for all nodes $\mathbf{x}_i \in \mathcal{N}_{\partial\tau \setminus e} := (\mathcal{N}_h \setminus \mathcal{N}_H) \cap (\partial\tau \setminus e)$. Let $R_{e,\tau}^T : \tilde{\Lambda}_h^e \rightarrow \tilde{\Lambda}_h^\tau$ be such extension. Conversely, we define the restriction operator $R_{e,\tau} : \tilde{\Lambda}_h^\tau \rightarrow \tilde{\Lambda}_h^e$ such that $R_{e,\tau} \nu_h(\mathbf{x}_i) = \nu_h(\mathbf{x}_i)$ for all nodes $\mathbf{x}_i \in \mathcal{N}_e := (\mathcal{N}_h \setminus \mathcal{N}_H) \cap e$.

Denote by $(\cdot, \cdot)_e$ the $L^2(e)$ inner product and define $S^\tau : \tilde{\Lambda}_h^\tau \rightarrow (\tilde{\Lambda}_h^\tau)'$, where $(\tilde{\Lambda}_h^\tau)'$ is the dual space of $\tilde{\Lambda}_h^\tau$, such that

$$(\mu_h^\tau, S^\tau \nu_h^\tau)_{\partial\tau} = \int_\tau \mathcal{A} \nabla T \mu_h^\tau \cdot \nabla T \nu_h^\tau d\mathbf{x} \quad \text{for all } \mu_h^\tau, \nu_h^\tau \in \tilde{\Lambda}_h^\tau.$$

Also let $S_{ee}^\tau : \tilde{\Lambda}_h^e \rightarrow (\tilde{\Lambda}_h^e)'$ be such that

$$(\tilde{\mu}_h^e, S_{ee}^\tau \tilde{\nu}_h^e)_e = (R_{e,\tau}^T \tilde{\mu}_h^e, S^\tau R_{e,\tau}^T \tilde{\nu}_h^e)_{\partial\tau} \quad \text{for all } \tilde{\mu}_h^e, \tilde{\nu}_h^e \in \tilde{\Lambda}_h^e,$$

Similarly we define $S_{e^c e}^\tau$, $S_{ee^c}^\tau$ and $S_{e^c e^c}^\tau$, related to the degrees of freedom on $e^c = \mathcal{N}_{\partial\tau \setminus e}$.

Let us introduce M_{ee}^τ by

$$(\tilde{\mu}_h^e, M_{ee}^\tau \tilde{\nu}_h^e)_e = \int_\tau \rho (TR_{e,\tau}^T \tilde{\mu}_h^e) (TR_{e,\tau}^T \tilde{\nu}_h^e) d\mathbf{x}$$

and define $\hat{S}_{ee}^\tau = \mathcal{H}^{-2} M_{ee}^\tau + S_{ee}^\tau$, where \mathcal{H} is the target precision of the method, that can be set by the user.

We finally consider the Schur complement

$$\tilde{S}_{ee}^\tau = S_{ee}^\tau - S_{ee^c}^\tau (S_{e^c e^c}^\tau)^{-1} S_{e^c e}^\tau,$$

and then

$$(18) \quad (\tilde{\nu}_h^e, \tilde{S}_{ee}^\tau \tilde{\nu}_h^e)_e \leq (\nu_h, S^\tau \nu_h) \quad \text{for all } \nu_h \in \tilde{\Lambda}_h^\tau \text{ such that } R_{e,\tau} \nu_h = \tilde{\nu}_h^e.$$

See [46] for a similar computation.

We are ready then to define a generalized eigenvalue problem that takes into account high contrast coefficients. For a given edge e shared by elements τ and τ' , find eigenpairs $(\alpha_i^e, \tilde{\psi}_{h,i}^e) \in (\mathbb{R}, \tilde{\Lambda}_h^e)$, where $\alpha_1^e \geq \alpha_2^e \geq \alpha_3^e \geq \dots \geq \alpha_{\mathcal{N}_e}^e > 1$, such that

$$(19) \quad (\hat{S}_{ee}^\tau + \hat{S}_{ee}^{\tau'}) \tilde{\psi}_{h,i}^e = \alpha_i^e (\tilde{S}_{ee}^\tau + \tilde{S}_{ee}^{\tau'}) \tilde{\psi}_{h,i}^e.$$

We impose that the eigenfunctions $\tilde{\mu}_{h,i}^e$ are orthonormal with respect to $(\cdot, (\hat{S}_{ee}^\tau + \hat{S}_{ee}^{\tau'}) \cdot)_e$. To see that all eigenvalues are greater than one, note from (18) and the above definitions that for all $\tilde{\psi}_h^e \in \tilde{\Lambda}_h^e$,

$$(\tilde{\psi}_h^e, \tilde{S}_{ee}^\tau \tilde{\psi}_h^e)_e \leq (R_{e,\tau}^T \tilde{\psi}_h^e, S^\tau R_{e,\tau}^T \tilde{\psi}_h^e) = (\tilde{\psi}_h^e, S_{ee}^\tau \tilde{\psi}_h^e)_e < (\tilde{\psi}_h^e, \hat{S}_{ee}^\tau \tilde{\psi}_h^e)_e,$$

where we recall that $R_{e,\tau}^T \tilde{\psi}_h^e$ is the extension of $\tilde{\psi}_h^e$ by zero.

Now we decompose $\tilde{\Lambda}_h^e := \tilde{\Lambda}_h^{e,\Delta} \oplus \tilde{\Lambda}_h^{e,\Pi}$ where for a given $\alpha_{\text{stab}} > 1$,

$$(20) \quad \tilde{\Lambda}_h^{e,\Delta} := \text{span}\{\tilde{\mu}_{h,i}^e : \alpha_i^e < \alpha_{\text{stab}}\}, \quad \tilde{\Lambda}_h^{e,\Pi} := \text{span}\{\tilde{\mu}_{h,i}^e : \alpha_i^e \geq \alpha_{\text{stab}}\}.$$

We remark that α_{stab} is chosen by the user and replaces α in the proof of Lemma 13, the counterpart of Lemma 5.

To define our ACMS–NLSD (*Approximated Component Mode Synthesis Non-Localized Spectral Decomposition*) method for high-contrast coefficients, let

$$(21) \quad \begin{aligned} \tilde{\Lambda}_h^\Pi &= \{\tilde{\mu}_h \in \tilde{\Lambda}_h : \tilde{\mu}_h|_e \in \tilde{\Lambda}_h^{e,\Pi} \text{ for all } e \in \partial\mathcal{T}_H\}, \\ \tilde{\Lambda}_h^\Delta &= \{\tilde{\mu}_h \in \tilde{\Lambda}_h : \tilde{\mu}_h|_e \in \tilde{\Lambda}_h^{e,\Delta} \text{ for all } e \in \partial\mathcal{T}_H\}. \end{aligned}$$

Note that $\Lambda_h = \Lambda_h^\Pi \oplus \tilde{\Lambda}_h^\Delta$, where

$$\Lambda_h^\Pi = \Lambda_h^0 \oplus \tilde{\Lambda}_h^\Pi$$

and Λ_h^0 is the set of functions on Λ_h which vanish on all nodes of $\mathcal{N}_h \setminus \mathcal{N}_H$. Denote

$$(\nu_h, S\mu_h)_{\partial\mathcal{T}_H} = \sum_{\tau \in \mathcal{T}_H} (\nu_h^\tau, S^\tau \mu_h^\tau)_{\partial\tau}.$$

We now introduce the ACMS–NLSD multiscale functions. For $\tau \in \mathcal{T}_H$, consider the operators $P^{\tau, \Delta}, P^\Delta : \Lambda_h \rightarrow \tilde{\Lambda}_h^\Delta$ as follows: Given $\mu_h \in \Lambda_h$, find $P^{\tau, \Delta} \mu_h \in \tilde{\Lambda}_h^\Delta$ and define P^Δ such that

$$(22) \quad (\tilde{\nu}_h^\Delta, SP^{\tau, \Delta} \mu_h)_{\partial\mathcal{T}_H} = (\tilde{\nu}_h^\Delta, S^\tau \mu_h)_{\partial\tau} \quad \text{for all } \tilde{\nu}_h^\Delta \in \tilde{\Lambda}_h^\Delta, \quad P^\Delta = \sum_{\tau \in \mathcal{T}_H} P^{\tau, \Delta}.$$

Consider $\Lambda_h^{\text{ms}, \Pi} = (I - P^\Delta) \Lambda_h^\Pi$. The ACMS–NLSD method is defined by: Find $\lambda_h^{\text{ms}, \Pi} \in \Lambda_h^{\text{ms}, \Pi}$ such that

$$(23) \quad (\nu_h^{\text{ms}, \Pi}, S\lambda_h^{\text{ms}, \Pi})_{\partial\mathcal{T}_H} = (\rho g, T\nu_h^{\text{ms}, \Pi}) \quad \text{for all } \nu_h^{\text{ms}, \Pi} \in \Lambda_h^{\text{ms}, \Pi}.$$

Note that

$$(\nu_h^{\text{ms}, \Pi}, S\lambda_h^{\text{ms}, \Pi})_{\partial\mathcal{T}_H} = \int_{\Omega} \mathcal{A} \nabla T\nu_h^{\text{ms}, \Pi} \cdot \nabla T\lambda_h^{\text{ms}, \Pi} d\mathbf{x} = \int_{\Omega} \rho g T\nu_h^{\text{ms}, \Pi} d\mathbf{x}.$$

Remark 3. A similar approach was followed by [34, 33], where different local eigenvalue problems are introduced to construct the approximation spaces. The analysis of the method however requires extra regularity of the coefficients, and the error estimate is not robust with respect to contrast.

Remark 4. Assume that \mathcal{A} is scalar and $\rho = \mathcal{A} \geq 1$. The generalized eigenvalue problem (19) was designed to guarantee that both the exponential decay of the multiscale function basis and local weighted Poincaré inequality holds,

$$\|v\|_{L^2_{\rho}(\tau \cup \tau')} \leq c\mathcal{H} \|v\|_{H^1_{\mathcal{A}}(\tau \cup \tau')},$$

without hidden constants depending of \mathcal{A} or on the contrast of \mathcal{A} . If the issue were just the exponential decay, it is possible to show from the analysis that we could have defined $\hat{S}_{ee}^\tau = S_{ee}^\tau$, furthermore, to show that the number of large eigenvalues is related to the number of high permeable channels crossing the edge e ; see [72, 73]. These eigenvectors are similar to functions that have value equal to one in one channel, zero value in the other channels, and smooth on the low permeable region. Related argument also applies to define subspaces where the weighted Poincaré inequality holds. In summary, we can control both the exponential decay and the local weighted Poincaré by using similar number of eigenvectors if using the

classical Poincaré inequality. As a consequence, the error estimate in terms of $\|f\|_{L^2_{1/\rho}}$ is a stronger result than in terms of $\|f\|_{L^2}$ and using similar number of multiscale function basis.

The counterpart of Lemma 1 follows.

Lemma 9. *Let $\tilde{\mu}_h^\Delta \in \tilde{\Lambda}_h^\Delta$. Then*

$$(24) \quad \|T\tilde{\mu}_h^\Delta\|_{L^2_\rho(\Omega)} \leq (9\alpha_{\text{stab}})^{1/2} \mathcal{H} |T\tilde{\mu}_h^\Delta|_{H^1_{\mathcal{A}}(\Omega)}.$$

Proof. We have for $\tau \in \mathcal{T}_H$,

$$\mathcal{H}^{-2} \|T\tilde{\mu}_h^\Delta\|_{L^2_\rho(\tau)}^2 \leq 3\mathcal{H}^{-2} \sum_{e \subset \partial\tau} \|TR_{e,\tau}^T \tilde{\mu}_h^{e,\Delta}\|_{L^2_\rho(\tau)}^2.$$

Fixing the edge e of both τ and τ' , we have

$$\begin{aligned} \mathcal{H}^{-2} \|TR_{e,\tau}^T \tilde{\mu}_h^{e,\Delta}\|_{L^2_\rho(\tau)}^2 + \mathcal{H}^{-2} \|TR_{e,\tau'}^T \tilde{\mu}_h^{e,\Delta}\|_{L^2_\rho(\tau')}^2 &\leq (\tilde{\mu}_h^{e,\Delta}, \hat{S}_{ee}^\tau \tilde{\mu}_h^{e,\Delta})_e + (\tilde{\mu}_h^{e,\Delta}, \hat{S}_{ee}^{\tau'} \tilde{\mu}_h^{e,\Delta})_e \\ &\leq \alpha_{\text{stab}} (\tilde{\mu}_h^{e,\Delta}, (\tilde{S}_{ee}^\tau + \tilde{S}_{ee}^{\tau'}) \tilde{\mu}_h^{e,\Delta})_e \leq \alpha_{\text{stab}} (|T\tilde{\mu}_h^\Delta|_{H^1_{\mathcal{A}}(\tau)}^2 + |T\tilde{\mu}_h^\Delta|_{H^1_{\mathcal{A}}(\tau')}^2) \end{aligned}$$

from (19), (20) and (18). By adding all $\tau \in \mathcal{T}_H$, the results follows. \square

Note that we added $\mathcal{H}^{-2} M_{ee}^\tau$ to define \hat{S}_{ee}^τ . This is necessary otherwise we might have a few modes that would make the local Poincaré's inequality constant in (24) too large.

Now we concentrate on the counterpart of Lemma 2.

Lemma 10. *Let $\mu_h \in \Lambda_h$ and let $\mu_h = \mu_h^\Pi + \tilde{\mu}_h^\Delta$. Then*

$$|T\mu_h^\Pi|_{H^1_{\mathcal{A}}(\Omega)} \leq (2 + 18\alpha_{\text{stab}})^{1/2} |T\mu_h|_{H^1_{\mathcal{A}}(\Omega)}.$$

Proof. We have

$$|T\mu_h^\Pi|_{H^1_{\mathcal{A}}(\Omega)}^2 \leq 2(|T\mu_h|_{H^1_{\mathcal{A}}(\Omega)}^2 + |T\tilde{\mu}_h^\Delta|_{H^1_{\mathcal{A}}(\Omega)}^2).$$

Consider the decomposition

$$\mu_h|_\tau = \mu_h^{\tau,0} + \sum_{e \subset \partial\tau} \tilde{\mu}_h^{\tau,e}$$

where $\mu_h^{\tau,0} \in \Lambda_h^0$ and $\tilde{\mu}_h^{\tau,e} = \tilde{\mu}_h^{\tau,e,\Pi} + \tilde{\mu}_h^{\tau,e,\Delta}$. Then

$$|T\tilde{\mu}_h^{\tau,\Delta}|_{H^1_{\mathcal{A}}(\tau)}^2 \leq 3 \sum_{e \subset \partial\tau} |TR_{e,\tau}^T \tilde{\mu}_h^{\tau,e,\Delta}|_{H^1_{\mathcal{A}}(\tau)}^2 = 3 \sum_{e \subset \partial\tau} (\tilde{\mu}_h^{\tau,e,\Delta}, S_{ee}^\tau \tilde{\mu}_h^{\tau,e,\Delta})_e.$$

Now we use that, if e is an edge of both τ and τ' ,

$$\left(\tilde{\mu}_h^{\tau,e,\Delta}, (S_{ee}^\tau + S_{ee}^{\tau'}) \tilde{\mu}_h^{\tau,e,\Delta} \right)_e \leq \alpha_{\text{stab}} \left(\tilde{\mu}_h^{\tau,e,\Delta}, (\tilde{S}_{ee}^\tau + \tilde{S}_{ee}^{\tau'}) \tilde{\mu}_h^{\tau,e,\Delta} \right)_e.$$

In addition, due to the orthogonality condition of the spaces $\tilde{\Lambda}_h^{e,\Delta}$ and $\tilde{\Lambda}_h^{e,\Pi}$ with respect to the inner product $(\cdot, (\tilde{S}_{ee}^\tau + \tilde{S}_{ee}^{\tau'})\cdot)_e$, and (18), we have

$$\left(\tilde{\mu}_h^{\tau,e,\Delta}, (\tilde{S}_{ee}^\tau + \tilde{S}_{ee}^{\tau'})\tilde{\mu}_h^{\tau,e,\Delta}\right)_e \leq \left(\tilde{\mu}_h^{\tau,e}, (\tilde{S}_{ee}^\tau + \tilde{S}_{ee}^{\tau'})\tilde{\mu}_h^{\tau,e}\right)_e \leq |T\mu_h^\tau|_{H_{\mathcal{A}}^1(\tau)}^2 + |T\mu_h^{\tau'}|_{H_{\mathcal{A}}^1(\tau')}^2.$$

Adding all terms together we obtain the result. \square

We now state the counterpart of the *Face Lemma* [71, Subsection 4.6.3]. The lemma follows directly from the definition of the generalized eigenvalue problem and properties of $\tilde{\Lambda}_h^{\tau,e,\Delta}$ and (18).

Lemma 11. *Let e be a common edge of $\tau, \tau' \in \mathcal{T}_H$, and $\tilde{\mu}_h^\Delta \in \tilde{\Lambda}_h^\Delta$. Then, defining $\tilde{\mu}_h^{e,\Delta} = R_{e,\tau}\tilde{\mu}_h^\Delta$ and $\tilde{\mu}_h^{\tau,\Delta} = \tilde{\mu}_h^\Delta|_{\partial\tau}$ it follows that*

$$|TR_{e,\tau}^T\tilde{\mu}_h^{e,\Delta}|_{H_{\mathcal{A}}^1(\tau)}^2 + |TR_{e,\tau'}^T\tilde{\mu}_h^{e,\Delta}|_{H_{\mathcal{A}}^1(\tau')}^2 \leq \alpha_{\text{stab}}(|T\tilde{\mu}_h^{\tau,\Delta}|_{H_{\mathcal{A}}^1(\tau)}^2 + |T\tilde{\mu}_h^{\tau',\Delta}|_{H_{\mathcal{A}}^1(\tau')}^2)$$

Proof. We have

$$\begin{aligned} |TR_{e,\tau}^T\tilde{\mu}_h^{e,\Delta}|_{H_{\mathcal{A}}^1(\tau)}^2 + |TR_{e,\tau'}^T\tilde{\mu}_h^{e,\Delta}|_{H_{\mathcal{A}}^1(\tau')}^2 &= (\tilde{\mu}_h^{e,\Delta}, S_{ee}^\tau\tilde{\mu}_h^{e,\Delta})_{\partial\tau} + (\tilde{\mu}_h^{e,\Delta}, S_{ee}^{\tau'}\tilde{\mu}_h^{e,\Delta})_{\partial\tau'} \\ &\leq \alpha_{\text{stab}}(\tilde{\mu}_h^{e,\Delta}, \tilde{S}_{ee}^\tau\tilde{\mu}_h^{e,\Delta})_{\partial\tau} + (\tilde{\mu}_h^{e,\Delta}, \tilde{S}_{ee}^{\tau'}\tilde{\mu}_h^{e,\Delta})_{\partial\tau'} \leq \alpha_{\text{stab}}(\tilde{\mu}_h^\Delta, S^\tau\tilde{\mu}_h^\Delta)_{\partial\tau} + (\tilde{\mu}_h^\Delta, S^{\tau'}\tilde{\mu}_h^\Delta)_{\partial\tau'}. \end{aligned}$$

\square

Theorem 12. *Let $\lambda_h = u_h|_{\partial\mathcal{T}_H}$, and $\lambda_h^{ms,\Pi}$ solution of (23). Then $\lambda_h - \lambda_h^{ms} \in \tilde{\Lambda}_h^\Delta$ and*

$$|u_h^{\mathbb{H}} - u_h^{ms,\Pi}|_{H_{\mathcal{A}}^1(\Omega)}^2 \leq 9\alpha_{\text{stab}}\mathcal{H}^2\|g\|_{L_\rho^2(\Omega)}^2.$$

Proof. First note that $\lambda_h - \lambda_h^{ms} \in \tilde{\Lambda}_h^\Delta$ since it follows from the Galerkin orthogonality that $s(\lambda_h - \lambda_h^{ms,\Pi}, \mu_h^{ms,\Pi}) = 0$ for all $\mu_h^{ms,\Pi} \in \Lambda_h^{ms}$. Using Lemma 9 we obtain

$$|u_h^{\mathbb{H}} - u_h^{ms,\Pi}|_{H_{\mathcal{A}}^1(\Omega)}^2 = (\rho g, T(\lambda_h - \lambda_h^{ms,\Pi})) \leq (9\alpha_{\text{stab}})^{1/2}\mathcal{H}\|g\|_{L_\rho^2(\Omega)}|T(\lambda_h - \lambda_h^{ms,\Pi})|_{H_{\mathcal{A}}^1(\Omega)},$$

and the result follows. \square

4.1. Decaying Results for High-Contrast coefficients. We next prove that $P^{K,\Delta}\nu_h$ with $K \in \mathcal{T}_H$ decay exponentially.

Lemma 13. *Let $\mu_h \in \Lambda_h$ and let $\tilde{\phi}_h^\Delta = P^{K,\Delta}\mu_h$ for some fixed element $K \in \mathcal{T}_H$. Then, for any integer $j \geq 1$,*

$$|T\tilde{\phi}_h^\Delta|_{H_{\mathcal{A}}^1(\mathcal{T}_H \setminus \mathcal{T}_{j+1}(K))}^2 \leq 9\alpha_{\text{stab}}|T\tilde{\phi}_h^\Delta|_{H_{\mathcal{A}}^1(\mathcal{T}_{j+2}(K) \setminus \mathcal{T}_j(K))}^2.$$

Proof. Following the steps of the proof of Lemma 5, we gather that

$$|T\tilde{\phi}_h^\Delta|_{H_{\mathcal{A}}^1(\mathcal{T}_H \setminus \mathcal{T}_{j+1}(K))}^2 \leq \sum_{\tau \in \mathcal{T}_{j+1}(K) \setminus \mathcal{T}_j(K)} |T\tilde{\nu}_h|_{H_{\mathcal{A}}^1(\tau)} |T\tilde{\phi}_h^\Delta|_{H_{\mathcal{A}}^1(\tau)},$$

where $\tilde{\nu}_h^\Delta \in \tilde{\Lambda}_h^\Delta$ is such that $\tilde{\nu}_h^\Delta|_{\partial\tau} = \tilde{\phi}_h^\Delta$ if $\tau \in \mathcal{T}_H \setminus \mathcal{T}_{j+1}(K)$, and $\tilde{\nu}_h^\Delta = 0$ on the remaining edges. If e is an edge of $\partial\tau$ and $\partial\tau'$, and χ_e the characteristic function of e , for $\tau \in \mathcal{T}_{j+1}(K) \setminus \mathcal{T}_j(K)$ and $\tau' \in \mathcal{T}_j(K) \setminus \mathcal{T}_{j-1}(K)$, then, for $\tilde{\mu}_h^{e,\Delta} = \tilde{\mu}_h^\Delta|_e$,

$$|T(\tilde{\mu}_h^\Delta)|_{H_{\mathcal{A}}^1(\tau)}^2 \leq 3 \sum_{e \subset \partial\tau} |T(\chi_e \tilde{\mu}_h^\Delta)|_{H_{\mathcal{A}}^1(\tau)}^2$$

and

$$\begin{aligned} |T(\chi_e \tilde{\mu}_h^\Delta)|_{H_{\mathcal{A}}^1(\tau)}^2 &= (\tilde{\mu}_h^{e,\Delta}, S_{ee}^\tau \tilde{\mu}_h^{e,\Delta})_e \leq \alpha_{\text{stab}}(\tilde{\mu}_h^{e,\Delta}, (\tilde{S}_{ee}^\tau + \tilde{S}_{ee}^{\tau'}) \tilde{\mu}_h^{e,\Delta})_e \\ &\leq \alpha_{\text{stab}}((\tilde{\mu}_h^\Delta, S^\tau \tilde{\mu}_h^\Delta)_{\partial\tau} + (\tilde{\mu}_h^\Delta, S^\tau \tilde{\mu}_h^\Delta)_{\partial\tau'}) = \alpha_{\text{stab}}(|T\tilde{\mu}_h^\Delta|_{H_{\mathcal{A}}^1(\tau)}^2 + |T\tilde{\mu}_h^\Delta|_{H_{\mathcal{A}}^1(\tau')}^2), \end{aligned}$$

where we have used (18). \square

Note that now the bound is in terms of $\mathcal{T}_{j+2}(K) \setminus \mathcal{T}_j(K)$ rather than $\mathcal{T}_{j+1}(K) \setminus \mathcal{T}_j(K)$. This means that the j in Corollary 6 is replaced below by the integer part of $(j+1)/2$.

Corollary 14. *Assume that $K \in \mathcal{T}_H$ and $\nu_h \in \Lambda_h$ and let $\tilde{\phi}_h^\Delta = P^{K,\Delta} \nu_h \in \tilde{\Lambda}_h^\Delta$. Then, for any integer $j \geq 1$,*

$$|T\tilde{\phi}_h^\Delta|_{H_{\mathcal{A}}^1(\mathcal{T}_H \setminus \mathcal{T}_{j+1}(K))}^2 \leq e^{-\frac{[(j+1)/2]}{1+9\alpha_{\text{stab}}}} |T\tilde{\phi}_h^\Delta|_{H_{\mathcal{A}}^1(\mathcal{T}_H)}^2.$$

where $[s]$ is the integer part of s .

Proof. Using Lemma 13 we have

$$\begin{aligned} |T\tilde{\phi}_h^\Delta|_{H_{\mathcal{A}}^1(\mathcal{T}_H \setminus \mathcal{T}_{j+1}(K))}^2 &\leq |T\tilde{\phi}_h^\Delta|_{H_{\mathcal{A}}^1(\mathcal{T}_H \setminus \mathcal{T}_j(K))}^2 \\ &\leq 9\alpha_{\text{stab}} |T\tilde{\phi}_h^\Delta|_{H_{\mathcal{A}}^1(\mathcal{T}_H \setminus \mathcal{T}_{j-1}(K))}^2 - 9\alpha_{\text{stab}} |T\tilde{\phi}_h^\Delta|_{H_{\mathcal{A}}^1(\mathcal{T}_H \setminus \mathcal{T}_{j+1}(K))}^2, \end{aligned}$$

and then

$$|T\tilde{\phi}_h^\Delta|_{H_{\mathcal{A}}^1(\mathcal{T}_H \setminus \mathcal{T}_{j+1}(K))}^2 \leq \frac{9\alpha_{\text{stab}}}{1+9\alpha_{\text{stab}}} |T\tilde{\phi}_h^\Delta|_{H_{\mathcal{A}}^1(\mathcal{T}_H \setminus \mathcal{T}_{j-1}(K))}^2 \leq e^{-\frac{1}{1+9\alpha_{\text{stab}}}} |T\tilde{\phi}_h^\Delta|_{H_{\mathcal{A}}^1(\mathcal{T}_H \setminus \mathcal{T}_{j-1}(K))}^2.$$

\square

Inspired by the exponential decay stated in Corollary 14, we define the operator $P^{\Delta,j}$ as follows. First, for a fixed $K \in \mathcal{T}_H$, let

$$\tilde{\Lambda}_h^{\Delta,K,j} = \{\tilde{\mu}_h \in \tilde{\Lambda}_h^\Delta : T\tilde{\mu}_h = 0 \text{ on } \mathcal{T}_H \setminus \mathcal{T}_j(K)\}.$$

For $\mu_h \in \Lambda_h$, define $P^{\Delta,K,j}\mu_h \in \tilde{\Lambda}_h^{K,j}$ such that

$$s(P^{\Delta,K,j}\mu_h, \tilde{\mu}_h) = s_K(\mu_h, \tilde{\mu}_h) \quad \text{for all } \tilde{\mu}_h \in \tilde{\Lambda}_h^{\Delta,K,j},$$

and let

$$(25) \quad P^{\Delta,j}\mu_h = \sum_{K \in \mathcal{T}_H} P^{\Delta,K,j}\mu_h.$$

Finally, define the approximation $\lambda_H^{\Pi,j} \in \Lambda_H^\Pi$ such that

$$(26) \quad s((I - P^{\Delta,j})\lambda_H^{\Pi,j}, (I - P^{\Delta,j})\mu_H^\Pi) = (\rho g, T(I - P^{\Delta,j})\mu_H^\Pi) \quad \text{for all } \mu_H^\Pi \in \Lambda_H^\Pi,$$

and then let $\lambda_h^{ms,\Pi,j} = (I - P^{\Delta,j})\lambda_H^{\Pi,j}$ and $u_h^{ms,\Pi,j} = T\lambda_h^{ms,\Pi,j}$. We name this the ACMS-LSD (*Approximated Component Mode Synthesis Localized Spectral Decomposition*) method.

We now analyze the approximation error of the method, starting by a technical result essential to obtain the final estimate.

Lemma 15. *Consider $\nu_h \in \Lambda_h$ and the operators P^Δ defined by (22) and $P^{\Delta,j}$ by (25) for $j > 1$. Then*

$$|T(P^\Delta - P^{\Delta,j})\nu_h|_{H_{\mathcal{A}}^1(\mathcal{T}_H)}^2 \leq (c_\gamma j)^2 (9\alpha_{\text{stab}})^2 e^{-\frac{[(j-1)/2]}{1+9\alpha_{\text{stab}}}} |T\nu_h|_{H_{\mathcal{A}}^1(\mathcal{T}_H)}^2,$$

where c_γ is as in (16).

Proof. Let $\tilde{\psi}_h^\Delta = (P^\Delta - P^{\Delta,j})\nu_h = \sum_{K \in \mathcal{T}_H} (P^{K,\Delta} - P^{K,\Delta,j})\nu_h$. For each $K \in \mathcal{T}_H$, let $\tilde{\psi}_h^{K,\Delta} \in \tilde{\Lambda}_h^\Delta$ be such that $\tilde{\psi}_h^{K,\Delta}|_e = 0$ if e is an edge of an element of $\mathcal{T}_j(K)$ and $\tilde{\psi}_h^{K,\Delta}|_e = \tilde{\psi}_h^\Delta|_e$, otherwise. We obtain

$$(27) \quad |T\tilde{\psi}_h^\Delta|_{H_{\mathcal{A}}^1(\mathcal{T}_H)}^2 = \sum_{K \in \mathcal{T}_H} \sum_{\tau \in \mathcal{T}_H} s_\tau(\tilde{\psi}_h^\Delta - \tilde{\psi}_h^{K,\Delta}, (P^K - P^{K,\Delta,j})\nu_h) + s_\tau(\tilde{\psi}_h^{\Delta,K}, (P^{K,\Delta} - P^{K,\Delta,j})\nu_h).$$

See that the second term of (27) vanishes since

$$\sum_{\tau \in \mathcal{T}_H} s_\tau(\tilde{\psi}_h^{K,\Delta}, (P^{K,\Delta} - P^{K,\Delta,j})\nu_h)_{\partial\tau} = \sum_{\tau \in \mathcal{T}_H} s_\tau(\tilde{\psi}_h^{K,\Delta}, P^{K,\Delta}\nu_h)_{\partial\tau} = 0.$$

For the first term of (17), as in Lemma 5,

$$\begin{aligned} & \sum_{\tau \in \mathcal{T}_H} s_\tau(\tilde{\psi}_h^\Delta - \tilde{\psi}_h^{K,\Delta}, (P^{K,\Delta} - P^{K,\Delta,j})\nu_h)_{\partial\tau} \\ & \leq \sum_{\tau \in \mathcal{T}_{j+1}(K)} |T(\tilde{\psi}_h^\Delta - \tilde{\psi}_h^{K,\Delta})|_{H_{\mathcal{A}}^1(\tau)} |T(P^{K,\Delta} - P^{K,\Delta,j})\nu_h|_{H_{\mathcal{A}}^1(\tau)} \\ & \leq 3\alpha_{\text{stab}}^{1/2} |T\tilde{\psi}_h^\Delta|_{H_{\mathcal{A}}^1(\mathcal{T}_{j+1}(K))} |T(P^{K,\Delta} - P^{K,\Delta,j})\nu_h|_{H_{\mathcal{A}}^1(\mathcal{T}_{j+1}(K))}. \end{aligned}$$

Let $\nu_h^{K,\Delta,j} \in \tilde{\Lambda}_h^{K,\Delta,j}$ be equal to zero on all faces of elements of $\mathcal{T}_H \setminus \mathcal{T}_j(K)$ and equal to $P^{K,\Delta} \nu_h$ otherwise. Using Galerkin best approximation property, Lemma 11 and Corollary 14, we obtain

$$\begin{aligned} |T(P^{K,\Delta} - P^{K,\Delta,j})\nu_h|_{H_{\mathcal{A}}^1(\mathcal{T}_{j+1}(K))}^2 &\leq |T(P^{K,\Delta} - P^{K,\Delta,j})\nu_h|_{H_{\mathcal{A}}^1(\mathcal{T}_H)}^2 \\ &\leq |T(P^{K,\Delta} \nu_h - \nu_h^{K,\Delta,j})|_{H_{\mathcal{A}}^1(\mathcal{T}_H)}^2 \leq 9\alpha_{\text{stab}} |TP^{K,\Delta} \nu_h|_{H_{\mathcal{A}}^1(\mathcal{T}_H \setminus \mathcal{T}_{j-1}(K))}^2 \\ &\leq 9\alpha_{\text{stab}} e^{-\frac{[(j-1)/2]}{1+9\alpha_{\text{stab}}}} |TP^{K,\Delta} \nu_h|_{H_{\mathcal{A}}^1(\mathcal{T}_H)}^2. \end{aligned}$$

We gather the above results to obtain

$$\begin{aligned} |T\tilde{\psi}_h^\Delta|_{H_{\mathcal{A}}^1(\mathcal{T}_H)}^2 &\leq 9\alpha_{\text{stab}} e^{-\frac{[(j-1)/2]}{2(1+2\alpha_{\text{stab}})}} \sum_{K \in \mathcal{T}_H} |T\tilde{\psi}_h^\Delta|_{H_{\mathcal{A}}^1(\mathcal{T}_{j+1}(K))} |TP^{K,\Delta} \nu_h|_{H_{\mathcal{A}}^1(\mathcal{T}_H)} \\ &\leq 9\alpha_{\text{stab}} e^{-\frac{[(j-1)/2]}{2(1+9\alpha_{\text{stab}})}} c_\gamma j |T\tilde{\psi}_h^\Delta|_{H_{\mathcal{A}}^1(\mathcal{T}_H)} \left(\sum_{K \in \mathcal{T}_H} |TP^{K,\Delta} \nu_h|_{H_{\mathcal{A}}^1(\mathcal{T}_H)}^2 \right)^{1/2}. \end{aligned}$$

We finally gather that

$$\begin{aligned} |TP^{K,\Delta} \nu_h|_{H_{\mathcal{A}}^1(\mathcal{T}_H)}^2 &= s(P^{K,\Delta} \nu_h, P^{K,\Delta} \nu_h)_{\partial \mathcal{T}_H} = s_K(P^{K,\Delta} \nu_h, \nu_h) \\ &= \int_K \mathcal{A} \nabla(TP^{K,\Delta} \nu_h) \cdot \nabla T \nu_h \, d\mathbf{x}, \end{aligned}$$

and from Cauchy–Schwarz, $|TP^{K,\Delta} \nu_h|_{H_{\mathcal{A}}^1(\mathcal{T}_H)} \leq |T \nu_h|_{H_{\mathcal{A}}^1(K)}$, we have

$$\sum_{K \in \mathcal{T}_H} |TP^{K,\Delta} \nu_h|_{H_{\mathcal{A}}^1(\mathcal{T}_H)}^2 \leq |T \nu_h|_{H_{\mathcal{A}}^1(\mathcal{T}_H)}^2.$$

□

Theorem 16. Define $u_h^{\mathbb{H}}$ by (3) and let $u_h^{ms,\Pi,j} = T(I - P^{\Delta,j})\lambda_H^{\Pi,j}$, where $\lambda_H^{\Pi,j}$ is as in (26). Then

$$|u_h^{\mathbb{H}} - u_h^{ms,\Pi,j}|_{H_{\mathcal{A}}^1(\mathcal{T}_H)} \leq \mathcal{H} \left(3(\alpha_{\text{stab}})^{1/2} + c_\gamma j 9\alpha_{\text{stab}} e^{-\left(\frac{[(j-1)/2]}{2(1+9\alpha_{\text{stab}})} - \log(c_{P,G}/\mathcal{H})\right)} \right) \|g\|_{L_\rho^2(\Omega)}.$$

Proof. First, from the triangle inequality,

$$|u_h^{\mathbb{H}} - u_h^{ms,\Pi,j}|_{H_{\mathcal{A}}^1(\mathcal{T}_H)} \leq |u_h^{\mathbb{H}} - u_h^{ms,\Pi}|_{H_{\mathcal{A}}^1(\mathcal{T}_H)} + |u_h^{ms,\Pi} - u_h^{ms,\Pi,j}|_{H_{\mathcal{A}}^1(\mathcal{T}_H)},$$

and for the first term we use Theorem 12. For the second term, we define $\hat{u}_h^{ms,\Pi,j} = T(I - P^{\Delta,j})\lambda_h^{ms,\Pi}$, and then

$$u_h^{ms} - \hat{u}_h^{ms,\Pi,j} = T(P - P^j)\lambda_h^{ms,\Pi}.$$

Relying on the Galerkin best approximation we gather from Lemma 15 that

$$|u_h^{ms} - u_h^{ms,\Pi,j}|_{H_{\mathcal{A}}^1(\mathcal{T}_H)}^2 \leq |u_h^{ms} - \hat{u}_h^{ms,\Pi,j}|_{H_{\mathcal{A}}^1(\mathcal{T}_H)}^2 \leq (c_\gamma j)^2 (9\alpha_{\text{stab}})^2 e^{-\frac{[(j-1)/2]}{(1+9\alpha_{\text{stab}})}} |T\lambda_h^{ms,\Pi}|_{H_{\mathcal{A}}^1(\mathcal{T}_H)}^2.$$

Since $u_h^{\text{ms}} = T\lambda_h^{\text{ms}}$ the result follow from Lemma 9 and the global Poincaré's inequality (10). \square

Remark 5. *The localization required for the a priori error estimate of the previous theorem depends just on the logarithm of the global Poincaré's inequality constant $c_{P,G}$ defined in (10). Furthermore, it is common in the literature to assume the global condition $a_{\min} \geq 1$ and $\rho = 1$, which implies $c_{P,G} = O(1)$. We can weaken this condition by choosing $\rho(\mathbf{x}) = a_-(\mathbf{x})$ for almost all $\mathbf{x} \in \Omega$ so that when the weighted Poincaré inequality holds [61, 58] then $c_{P,G} = O(1)$; a simple example of such a case is when Ω is composed of several inclusions with small permeabilities and surrounded by a material with a large permeability.*

Remark 6. *The complexity of the proposed method depends on the number of eigenvalues of (19) below a threshold α_{stab} associated to each edge e . There are several works on the literature discussing this issue for similar eigenvalues problems [26, 73, 72] and the number is related to the amount of channels of high permeability crossing the edge e . For the numerical experiments tested in [45], just one eigenvalue per edge was enough for $\mathcal{H} = H$, $\mathcal{H} = H/2$ and $\mathcal{H} = H/4$ with $\alpha_{\text{stab}} = 1.5$*

5. SPECTRAL MULTISCALE PROBLEMS INSIDE SUBSTRUCTURES

Recall the decomposition $u_h = u_h^B + u_h^{\mathbb{H}}$, and so far we derived a scheme that approximates $u_h^{\mathbb{H}}$ only. From (3), we gather that u_h^B is defined locally. Fixing an element $\tau \in \mathcal{T}_H$, we introduce a multiscale method by first building the approximation space $V_\tau^{\text{ms}} := \text{span}\{\psi_h^1, \psi_h^2, \dots, \psi_h^{N_\tau}\}$ generated by the following generalized eigenvalue problem: Find the eigenpairs $(\alpha_i, \psi_h^i) \in (\mathbb{R}, V_h^B(\tau))$ such that

$$a_\tau(v_h, \psi_h^i) = \lambda_i(\rho v_h, \psi_h^i)_\tau \quad \text{for all } v_h \in V_h^B(\tau)$$

where

$$a_\tau(v_h, \psi_h^i) = \int_\tau \mathcal{A} \nabla v_h \cdot \nabla \psi_h^i d\mathbf{x} \quad \text{and} \quad (\rho v_h, \psi_h^i)_\tau = \int_\tau \rho v_h \psi_h^i d\mathbf{x}$$

and $0 < \lambda_1 \leq \lambda_2 \leq \dots \leq \lambda_{N_\tau} < 1/\mathcal{H}^2$ and $\lambda_{N_\tau+1} \geq 1/\mathcal{H}^2$. Again, \mathcal{H} is the user defined target accuracy target. For instance $\mathcal{H} = H$ or $\mathcal{H} = h^r, 0 < r \leq 1$. The local multiscale problem is defined by: Find $u_h^{B,\text{ms}} \in V_h^{\text{ms}}$ such that

$$a_\tau(u_h^{B,\text{ms}}, v_h) = (\rho g, v_h)_\tau \quad \text{for all } v_h \in V_h^{B,\text{ms}}.$$

It then follows that

$$|u_h^B - u_h^{B,\text{ms}}|_{H_{\mathcal{A}}^1(\tau)}^2 = (\rho g, u_h^B - u_h^{B,\text{ms}})_\tau \leq \mathcal{H} |u_h^B - u_h^{B,\text{ms}}|_{H_{\mathcal{A}}^1(\tau)} \|g\|_{L_\rho^2(\tau)}$$

and $|u_h^B - u_h^{B,\text{ms}}|_{H_{\mathcal{A}}^1(\tau)} \leq \mathcal{H} \|g\|_{L_\rho^2(\tau)}$. See [46, Section 4] for a similar computation.

H/h	α_1^e	α_2^e	α_3^e	α_4^e	α_5^e	α_6^e	α_7^e
8	1.7196	1.1503	1.0134	1.0013	1.0001	1.0000	1.0000
16	2.2140	1.3272	1.0525	1.0109	1.0015	1.0002	1.0000
32	2.8065	1.5558	1.1199	1.0354	1.0078	1.0019	1.0004

TABLE 1. The 7th largest eigenvalues of the eigenvalue problem (19) with $\mathcal{H} = H$.

6. NUMERICAL EXPERIMENT TESTS

Let $\Omega = (0, 1)^2$ and consider a Cartesian mesh of $2^M \times 2^M$ coarse squares, and then subdivide each square into $2^{N-M} \times 2^{N-M}$ equal fine squares and then subdivide further into two 45-45-90 triangular elements. Denote $H = 2^{-M}$ and $h = 2^{-N}$ as the sizes of the coarse and the fine elements, respectively. We remind that $\alpha_{\text{stab}} > 1$, introduced in (20), controls how fast the multiscale basis functions decays exponentially (see Corollary 14), while \mathcal{H} is the target precision of the method (see Theorem 12), and was introduced in the definition of \hat{S}_{ee}^τ to build the generalized eigenvalue problem (19). To obtain an effective decay we should choose α_{stab} close to one, while keeping the number of eigenvalues above α_{stab} small. We assume the bubble solution u_h^B is computed exactly, therefore, $u_h^{\mathbb{H}} - u_h^{ms, \Pi} = u_h - u_h^{ms}$ and $u_h^{\mathbb{H}} - u_h^{ms, \Pi, j} = u_h - u_h^{ms, j}$ where $u_h^{ms, j} = u_h^B + u_h^{ms, j}$.

For the first numerical test, we find a judicious choice of α_{stab} . We consider $\mathcal{A}(\mathbf{x}) = 1$ and $\rho(\mathbf{x}) = 1$ and $\mathcal{H} = H$ for different values of H/h . Table 1 shows the seven largest generalized eigenvalues of (19). We consider the case where the coarse edge e of $\partial\mathcal{T}_H \setminus \partial\Omega$ is shared by the coarse elements τ and τ' of \mathcal{T}_H where τ and τ' do not share an edge with $\partial\Omega$. This is the coarse edge case which the eigenvalues are the largest. We choose α_{stab} so that we can remove the weak corner singularities. The choices $\alpha_{\text{max}} = 1.5$ and 1.3 are good compromises between the fast decay of the multiscale basis functions while keeping the number of selected large eigenvalues small. When $\mathcal{A}(\mathbf{x})$ is highly heterogeneous or has high-contrast coefficients channels crossing the coarse edge e , very large eigenvalues might appear on the generalized eigenvalue problem (19), and for $\alpha_{\text{stab}} = 1.5$ or 1.3 these large eigenvalues will also be selected. See in Table 1 that the smallest eigenvalues converge fast to one.

The second numerical test is borrowed from [45]. We consider the distribution of $\mathcal{A}(\mathbf{x})$ to be a channel on the form of a **H**. We examine the exponential decay of the multiscale basis functions under the presence of large coefficient on the **H**-shape region.

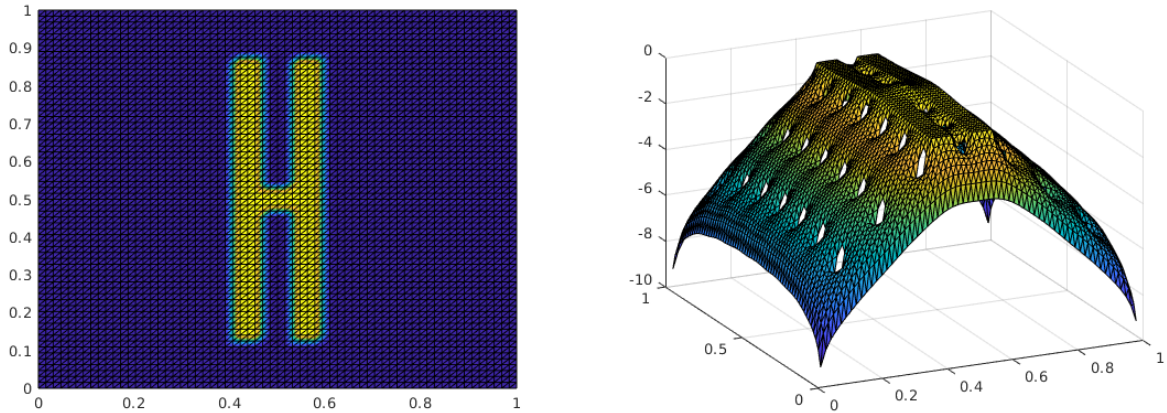


FIGURE 1. On the left, the distribution of the coefficient for a 8×8 subdomain decomposition. On the right, the log-normal plot of the multiscale basis functions without adaptivity. Note that there is no exponential decay whatsoever.

We assume that $\mathcal{A}(\mathbf{x})$ is scalar and that $\rho(\mathbf{x}) = \mathcal{A}(\mathbf{x})$. The distribution of $\mathcal{A}(\mathbf{x})$ is shown on the left of Figure 1, where $\mathcal{A} = 100$ inside the **H**-shape region and $\mathcal{A} = 1$ outside. Let $N = 6$ and $M = 3$. This distribution of the coefficients \mathcal{A} has the property that $\mathcal{A}(1/2, 1/2) = 100$ at the corner coarse node $\mathbf{x} = (1/2, 1/2)$ and $\mathcal{A} = 1$ at the remaining corner coarse nodes. The right Figure 1 shows the (lack of) decay (in the log-normal scale) of the multiscale basis function associated to the coarse node $\mathbf{x} = (1/2, 1/2)$ without the eigenfunctions. We can see that this multiscale basis function does not decay fast away from $\mathcal{A}(1/2, 1/2)$ on the **H**-shape region. The presence of the white holes in this picture is because the value of the function is closed to zero since this multiscale basis function vanishes at all coarse nodes but at $(1/2, 1/2)$. The reason for this non-decay is due to that this multiscale basis function “wants” to have small energy, therefore, “wants” to be near one on the **H**-shape region, where \mathcal{A} is large. We now consider the adaptive case with $\alpha_{\text{stab}} = 1.5$. Figure 2 shows the exponential decay when $\mathcal{H} = H$, as predicted by the theory.

In the third numerical experiment we keep the same distribution of coefficients in Figure 1 with $N = 6$ and $M = 3$. To make the problem a little more complicated, we multiply \mathcal{A} and ρ in each element by independently uniform random distributions between zero and one. Similarly, we let f to be constant in each element given by another independently uniformly random distributions between zero and one. Table 2 shows the energy errors for different values of \mathcal{H} . We also include the total number of edges functions required for a \mathcal{H} tolerance. We take $\alpha_{\text{stab}} = 1.5$. We note that there are 49 interior coarse corners nodes,

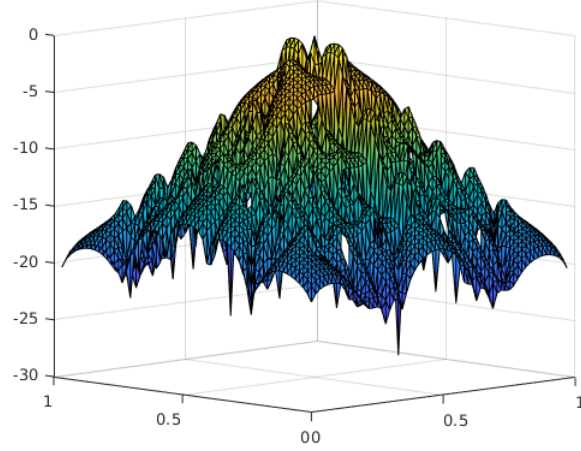


FIGURE 2. Log-normal plot showing the decay of a multiscale basis functions with adaptivity, for $\mathcal{H} = H$.

\mathcal{H}	$ u_h - u_h^{\text{ms}} _{H_{\mathcal{A}}^1}$	$\frac{ u_h - u_h^{\text{ms}} _{H_{\mathcal{A}}^1}}{ u_h _{H_{\mathcal{A}}^1}}$	$\frac{ u_h - u_h^{\text{ms}} _{H_{\mathcal{A}}^1}}{\ f\ _{L_{\rho}^2}}$	Neigs
1/8	0.0095	0.0083	0.0079	78
1/16	0.0064	0.0056	0.0053	92
1/32	0.0025	0.0022	0.0021	112
1/64	0.0014	0.0012	0.0011	226

TABLE 2. The energy errors for different accuracy targets \mathcal{H} . The last column shows Neigs (the total number of multiscale edges functions). We let $\alpha_{\text{stab}} = 1.5$.

112 interior coarse edges, and 7 fine nodes per open coarse edges. By taking $\mathcal{H} = H$, the number of edge multiscale basis functions is smaller than the number of coarse edges.

In Table 3 we provide the energy error for different values of α_{stab} ; by adding few edge multiscale basis functions on the approximation space, we see a dramatic improvement on the energy error. In Table 4 we refine the mesh and consider $H = 1/16$, $H/h = 16$, $\mathcal{H} = H$ and compute the energy error for different values of localization j ; here, $j = -1$ means the classical Adaptive BDDC [39]; also See that a small localization j is sufficient for α_{stab} sufficiently small.

α_{stab}	$ u_h - u_h^{\text{ms}} _{H_A^1}$	Neigs
100	0.299	0
10	0.0964	8
2	0.0204	14
1.5	0.0107	79
1.3	0.0084	103
1.2	0.0075	112
1.1	0.0063	171

TABLE 3. The energy errors $\mathcal{H} = H$ and different values of α_{stab} .

$\alpha_{\text{stab}}(\text{Neigs}) \setminus j$	-1	0	1	2	3
10(24)	0.6913	0.6543	0.2562	0.0547	0.0305
3 (55)	0.6797	0.5236	0.2149	0.0378	0.0154
2(416)	0.6562	0.1225	0.0056	0.0057	0.0057
1.1(1286)	0.5908	0.0031	0.0022	0.0022	0.0022

TABLE 4. The energy errors $u_h - u_h^{\text{ms},j}$ with $\mathcal{H} = H, H = 1/16, H/h = 1/16$ and different values of α_{stab} and localization j .

REFERENCES

- [1] Araya, Rodolfo, Harder, Christopher, Paredes, Diego, and Valentin, Frédéric. Multiscale hybrid-mixed method. *SIAM J. Numer. Anal.*, 51(6):3505–3531, 2013.
- [2] Babuska, Ivo and Lipton, Robert. Optimal local approximation spaces for generalized finite element methods with application to multiscale problems. *Multiscale Model. Simul.*, 9(1):373–406, 2011.
- [3] Babuška, Ivo, Caloz, Gabriel, and Osborn, John E. Special finite element methods for a class of second order elliptic problems with rough coefficients. *SIAM J. Numer. Anal.*, 31(4):945–981, 1994.
- [4] Beirão da Veiga, L., Pavarino, L. F., Scacchi, S., Widlund, O. B., and Zampini, S. Adaptive selection of primal constraints for isogeometric BDDC deluxe preconditioners. *SIAM J. Sci. Comput.*, 39(1):A281–A302, 2017.
- [5] Petter E. Bjø rstad and Olof B. Widlund. Solving elliptic problems on regions partitioned into substructures. In *Elliptic problem solvers, II (Monterey, Calif., 1983)*, pages 245–255. Academic Press, Orlando, FL, 1984.
- [6] Bourquin, F. Component mode synthesis and eigenvalues of second order operators: discretization and algorithm. *RAIRO Modél. Math. Anal. Numér.*, 26(3):385–423, 1992.

- [7] Bourquin, Frédéric. Analysis and comparison of several component mode synthesis methods on one-dimensional domains. *Numer. Math.*, 58(1):11–33, 1990.
- [8] Bramble, J. H., Pasciak, J. E., and Schatz, A. H. The construction of preconditioners for elliptic problems by substructuring. i. *Math. Comp.*, 47(175):103–134, 1986.
- [9] Calvo, Juan G. and Widlund, Olof B. An adaptive choice of primal constraints for BDDC domain decomposition algorithms. *Electron. Trans. Numer. Anal.*, 45:524–544, 2016.
- [10] Chu, C.-C., Graham, I. G., and Hou, T.-Y. A new multiscale finite element method for high-contrast elliptic interface problems. *Math. Comp.*, 79(272):1915–1955, 2010.
- [11] Eric T. Chung, Yalchin Efendiev, and Wing Tat Leung. Constraint energy minimizing generalized multiscale finite element method. *Comput. Methods Appl. Mech. Engrg.*, 339:298–319, 2018.
- [12] Chung, Eric T, Efendiev, Yalchin, and Leung, Wing Tat. Constraint energy minimizing generalized multiscale finite element method in the mixed formulation. *Computational Geosciences*, 22(3):677–693, 2018.
- [13] Craig, Roy R and Bampton, Mervyn CC. Coupling of substructures for dynamic analyses. *AIAA journal*, 6(7):1313–1319, 1968.
- [14] C. Dohrmann and C. Pechstein. Modern decomposition solvers - BDDC, deluxe scaling, and an algebraic approach, 2013. Slides to a talk at NuMa Seminar, JKU Linz, Linz, Austria, December 10.
- [15] Dohrmann, Clark R. A preconditioner for substructuring based on constrained energy minimization. *SIAM J. Sci. Comput.*, 25(1):246–258, 2003.
- [16] Dolean, Victorita, Nataf, Frédéric, Scheichl, Robert, and Spillane, Nicole. Analysis of a two-level Schwarz method with coarse spaces based on local Dirichlet-to-Neumann maps. *Comput. Methods Appl. Math.*, 12(4):391–414, 2012.
- [17] Maksymilian Dryja and Marcus Sarkis. Technical tools for boundary layers and applications to heterogeneous coefficients. In *Domain decomposition methods in science and engineering XIX*, volume 78 of *Lect. Notes Comput. Sci. Eng.*, pages 205–212. Springer, Heidelberg, 2011.
- [18] Dryja, Maksymilian, Sarkis, Marcus V., and Widlund, Olof B. Multilevel Schwarz methods for elliptic problems with discontinuous coefficients in three dimensions. *Numer. Math.*, 72(3):313–348, 1996.
- [19] Dryja, Maksymilian, Smith, Barry F., and Widlund, Olof B. Schwarz analysis of iterative substructuring algorithms for elliptic problems in three dimensions. *SIAM J. Numer. Anal.*, 31(6):1662–1694, 1994.
- [20] E, Weinan and Engquist, Bjorn. The heterogeneous multiscale methods. *Commun. Math. Sci.*, 1(1):87–132, 2003.
- [21] E, Weinan and Ming, Pingbing. Analysis of multiscale methods. *J. Comput. Math.*, 22(2):210–219, 2004.
- [22] Efendiev, Y., Galvis, J., Lazarov, R., Moon, M., and Sarkis, M. Generalized multiscale finite element method. symmetric interior penalty coupling. *J. Comput. Phys.*, 255:1–15, 2013.
- [23] Efendiev, Yalchin, Galvis, Juan, Lazarov, Raytcho, and Willems, Joerg. Robust domain decomposition preconditioners for abstract symmetric positive definite bilinear forms. *ESAIM Math. Model. Numer. Anal.*, 46(5):1175–1199, 2012.
- [24] Farhat, Charbel, Lesoinne, Michael, and Pierson, Kendall. A scalable dual-primal domain decomposition method. *Numer. Linear Algebra Appl.*, 7(7-8):687–714, 2000. Preconditioning techniques for large sparse matrix problems in industrial applications (Minneapolis, MN, 1999).

- [25] Galvis, Juan and Efendiev, Yalchin. Domain decomposition preconditioners for multiscale flows in high-contrast media. *Multiscale Model. Simul.*, 8(4):1461–1483, 2010.
- [26] Galvis, Juan and Efendiev, Yalchin. Domain decomposition preconditioners for multiscale flows in high contrast media: reduced dimension coarse spaces. *Multiscale Model. Simul.*, 8(5):1621–1644, 2010.
- [27] Johnny Guzmán, Manuel A. Sánchez, and Marcus Sarkis. A finite element method for high-contrast interface problems with error estimates independent of contrast. *J. Sci. Comput.*, 73(1):330–365, 2017.
- [28] Harder, Christopher, Madureira, Alexandre L., and Valentin, Frédéric. A hybrid-mixed method for elasticity. *ESAIM, Math. Model. Numer. Anal.*, 50(2):311–336, 2016.
- [29] Harder, Christopher, Paredes, Diego, and Valentin, Frédéric. A family of multiscale hybrid-mixed finite element methods for the Darcy equation with rough coefficients. *J. Comput. Phys.*, 245:107–130, 2013.
- [30] Heinlein, A., Hetmaniuk, U., Klawonn, A., and Rheinbach, O. The approximate component mode synthesis special finite element method in two dimensions: parallel implementation and numerical results. *J. Comput. Appl. Math.*, 289:116–133, 2015.
- [31] Hellman, Fredrik and Målqvist, Axel. Contrast independent localization of multiscale problems. *Multiscale Modeling & Simulation*, 15(4):1325–1355, 2017.
- [32] Patrick Henning and Daniel Peterseim. Oversampling for the multiscale finite element method. *Multiscale Model. Simul.*, 11(4):1149–1175, 2013.
- [33] Hetmaniuk, Ulrich and Klawonn, Axel. Error estimates for a two-dimensional special finite element method based on component mode synthesis. *Electron. Trans. Numer. Anal.*, 41:109–132, 2014.
- [34] Hetmaniuk, Ulrich L. and Lehoucq, Richard B. A special finite element method based on component mode synthesis. *M2AN Math. Model. Numer. Anal.*, 44(3):401–420, 2010.
- [35] Hou, Thomas Y., Wu, Xiao-Hui, and Cai, Zhiqiang. Convergence of a multiscale finite element method for elliptic problems with rapidly oscillating coefficients. *Math. Comp.*, 68(227):913–943, 1999.
- [36] Hughes, T. J. R. and Sangalli, G. Variational multiscale analysis: the fine-scale Green’s function, projection, optimization, localization, and stabilized methods. *SIAM J. Numer. Anal.*, 45(2):539–557, 2007.
- [37] Hughes, Thomas J. R., Feijóo, Gonzalo R., Mazzei, Luca, and Quincy, Jean-Baptiste. The variational multiscale method—a paradigm for computational mechanics. *Comput. Methods Appl. Mech. Engrg.*, 166(1-2):3–24, 1998.
- [38] Hurty, Walter C. Vibrations of structural systems by component mode synthesis. *Journal of the Engineering Mechanics Division*, 86(4):51–70, 1960.
- [39] Kim, Hyea Hyun and Chung, Eric T. A BDDC algorithm with enriched coarse spaces for two-dimensional elliptic problems with oscillatory and high contrast coefficients. *Multiscale Model. Simul.*, 13(2):571–593, 2015.
- [40] Klawonn, A., Radtke, P., and Rheinbach, O. FETI-DP methods with an adaptive coarse space. *SIAM J. Numer. Anal.*, 53(1):297–320, 2015.
- [41] Klawonn, Axel, Kühn, Martin, and Rheinbach, Oliver. Adaptive coarse spaces for FETI-DP in three dimensions. *SIAM J. Sci. Comput.*, 38(5):A2880–A2911, 2016.

- [42] Klawonn, Axel, Widlund, Olof B., and Dryja, Maksymilian. Dual-primal FETI methods for three-dimensional elliptic problems with heterogeneous coefficients. *SIAM J. Numer. Anal.*, 40(1):159–179, 2002.
- [43] A. V. Knyazev. A preconditioned conjugate gradient method for eigenvalue problems and its implementation in a subspace. In *Numerical treatment of eigenvalue problems, Vol. 5 (Oberwolfach, 1990)*, volume 96 of *Internat. Ser. Numer. Math.*, pages 143–154. Birkhäuser, Basel, 1991.
- [44] Knyazev, A. V. and Skorokhodov, A. L. On exact estimates of the convergence rate of the steepest ascent method in the symmetric eigenvalue problem. *Linear Algebra Appl.*, 154/156:245–257, 1991.
- [45] Madureira, Alexandre and Sarkis, Marcus. Robust model reduction discretizations based on adaptive BDDC techniques. In *Domain decomposition methods in science and engineering XXV. Selected papers based on the presentations at the 25th international conference on domain decomposition methods, Memorial University of Newfoundland, in St. John's, Newfoundland and Labrador, Canada, July 23–27, 2018*, pages 41–52. Cham: Springer, 2020.
- [46] Madureira, Alexandre L. and Sarkis, Marcus. Hybrid Localized Spectral Decomposition for Multiscale Problems. *SIAM J. Numer. Anal.*, 59(2):829–863, 2021.
- [47] Jan Mandel and Bedřich Sousedík. Adaptive coarse space selection in the BDDC and the FETI-DP iterative substructuring methods: optimal face degrees of freedom. In *Domain decomposition methods in science and engineering XVI*, volume 55 of *Lect. Notes Comput. Sci. Eng.*, pages 421–428. Springer, Berlin, 2007.
- [48] Mandel, Jan and Dohrmann, Clark R. Convergence of a balancing domain decomposition by constraints and energy minimization. *Numer. Linear Algebra Appl.*, 10(7):639–659, 2003. Dedicated to the 70th birthday of Ivo Marek.
- [49] Mandel, Jan and Sousedík, Bedřich. Adaptive selection of face coarse degrees of freedom in the BDDC and the FETI-DP iterative substructuring methods. *Comput. Methods Appl. Mech. Engrg.*, 196(8):1389–1399, 2007.
- [50] Målqvist, Axel. Multiscale methods for elliptic problems. *Multiscale Model. Simul.*, 9(3):1064–1086, 2011.
- [51] Målqvist, Axel, Henning, Patrick, and Hellman, Fredrik. Multiscale mixed finite elements. *Discrete Contin. Dyn. Syst. Ser. S*, 9(5):1269–1298, 2016.
- [52] Målqvist, Axel and Peterseim, Daniel. Localization of elliptic multiscale problems. *Math. Comp.*, 83(290):2583–2603, 2014.
- [53] A. Målqvist and D. Peterseim. *Numerical homogenization by localized orthogonal decomposition*, volume 5 of *SIAM Spotlights*. Society for Industrial and Applied Mathematics (SIAM), Philadelphia, PA, [2021] ©2021.
- [54] Oh, D-S., Widlund, O. B., Zampini, S., and Dohrmann, C. R. BDDC algorithms with deluxe scaling and adaptive selection of primal constraints for raviart–thomas vector fields. *Math. Comp.*, 2017.
- [55] Owjadi, Houman, Zhang, Lei, and Berlyand, Leonid. Polyharmonic homogenization, rough polyharmonic splines and sparse super-localization. *ESAIM Math. Model. Numer. Anal.*, 48(2):517–552, 2014.
- [56] Clemens Pechstein and Clark R. Dohrmann. A unified framework for adaptive BDDC. *Electron. Trans. Numer. Anal.*, 46:273–336, 2017.

- [57] Pechstein, Clemens. *Finite and boundary element tearing and interconnecting solvers for multiscale problems*, volume 90 of *Lecture Notes in Computational Science and Engineering*. Springer, Heidelberg, 2013.
- [58] Pechstein, Clemens, Sarkis, Marcus, and Scheichl, Robert. New theoretical coefficient robustness results for FETI-DP. In *Domain decomposition methods in science and engineering XX. Selected papers based on the presentations of the 20th international conference on domain decomposition, San Diego, CA, USA, February 9–13, 2011*, pages 313–320. Berlin: Springer, 2013.
- [59] Pechstein, Clemens and Scheichl, Robert. Analysis of FETI methods for multiscale PDEs. *Numer. Math.*, 111(2):293–333, 2008.
- [60] Pechstein, Clemens and Scheichl, Robert. Analysis of FETI methods for multiscale PDEs. part II: interface variation. *Numer. Math.*, 118(3):485–529, 2011.
- [61] Pechstein, Clemens and Scheichl, Robert. Weighted Poincaré inequalities. *IMA J. Numer. Anal.*, 33(2):652–686, 2013.
- [62] Peterseim, Daniel and Scheichl, Robert. Robust numerical upscaling of elliptic multiscale problems at high contrast. *Comput. Methods Appl. Math.*, 16(4):579–603, 2016.
- [63] Quarteroni, Alfio and Valli, Alberto. *Domain decomposition methods for partial differential equations*. Numerical Mathematics and Scientific Computation. The Clarendon Press, Oxford University Press, New York, 1999. Oxford Science Publications.
- [64] Raviart, P.-A. and Thomas, J. M. Primal hybrid finite element methods for 2nd order elliptic equations. *Math. Comp.*, 31(138):391–413, 1977.
- [65] Sangalli, Giancarlo. Capturing small scales in elliptic problems using a residual-free bubbles finite element method. *Multiscale Model. Simul.*, 1(3):485–503 (electronic), 2003.
- [66] Sarkis, Marcus. Nonstandard coarse spaces and Schwarz methods for elliptic problems with discontinuous coefficients using non-conforming elements. *Numer. Math.*, 77(3):383–406, 1997.
- [67] Sarkis, Marcus and Versieux, Henrike. Convergence analysis for the numerical boundary corrector for elliptic equations with rapidly oscillating coefficients. *SIAM J. Numer. Anal.*, 46(2):545–576, 2008.
- [68] Scheichl, Robert, Vassilevski, Panayot S., and Zikatanov, Ludmil T. Weak approximation properties of elliptic projections with functional constraints. *Multiscale Model. Simul.*, 9(4):1677–1699, 2011.
- [69] Spillane, N., Dolean, V., Hauret, P., Nataf, F., Pechstein, C., and Scheichl, R. Abstract robust coarse spaces for systems of PDEs via generalized eigenproblems in the overlaps. *Numer. Math.*, 126(4):741–770, 2014.
- [70] Spillane, Nicole, Dolean, Victorita, Hauret, Patrice, Nataf, Frédéric, and Rixen, Daniel J. Solving generalized eigenvalue problems on the interfaces to build a robust two-level FETI method. *C. R. Math. Acad. Sci. Paris*, 351(5-6):197–201, 2013.
- [71] Toselli, Andrea and Widlund, Olof. *Domain decomposition methods—algorithms and theory*, volume 34 of *Springer Series in Computational Mathematics*. Springer-Verlag, Berlin, 2005.
- [72] Yi Yu and Marcus Sarkis. A family of nonoverlapping spectral additive Schwarz methods (NOSAS) and their economic versions. *J. Comput. Appl. Math.*, 443:Paper No. 115734, 21, 2024.

- [73] Yu, Yi, Dryja, Maksymilian, and Sarkis, Marcus. From additive average Schwarz methods to nonoverlapping spectral additive Schwarz methods. *SIAM Journal on Numerical Analysis*, 59(5):2608–2638, 2021.

LABORATÓRIO NACIONAL DE COMPUTAÇÃO CIENTÍFICA, PETRÓPOLIS - RJ, BRAZIL

FUNDAÇÃO GETÚLIO VARGAS, RIO DE JANEIRO - RJ, BRAZIL

Email address: alm@lncc.br, alexandre.madureira@fgv.br

MATHEMATICAL SCIENCES DEPARTMENT WORCESTER POLYTECHNIC INSTITUTE, USA

Email address: msarkis@wpi.edu